Focused fields of given power with maximum electric field components

H. P. Urbach* and S. F. Pereira
Optics Research Group, Department of Imaging Science and Technology, Delft University of Technology, P.O. Box 5046, 2600 GA Delft, The Netherlands

(Received 27 August 2008; revised manuscript received 24 October 2008; published 28 January 2009)

Closed formulas are derived for the field in the focal region of a diffraction limited lens, such that the electric field component in a given direction at the focal point is larger than that of all other focused fields with the same power in the entrance pupil of the lens. Furthermore, closed formulas are derived for the corresponding optimum field distribution in the lens pupil. Focused fields with maximum longitudinal or maximum transverse are considered in detail. The latter field is similar, but not identical, to the focused linearly polarized plane wave.

DOI: 10.1103/PhysRevA.79.013825 PACS number(s): 42.30.Va, 42.25.Fx, 42.79.Hp, 42.79.Bh

I. INTRODUCTION

When a linearly polarized plane wave is focused by a diffraction-limited lens, the intensity distribution in the focal plane is in the scalar theory the well-known Airy pattern. However, when the lens has high numerical aperture, the rotation of polarization must be accounted for and the vector diffraction theory of Ignatowsky [1,2] and Richards and Wolf [3,4] has to be applied to obtain the field distribution in the focal region. We then obtain three electric and three magnetic field components in the focal region. When the beam in the lens aperture is uniformly linearly polarized plane wave, the dominant electric field component in the focal region is found to be parallel to the polarization direction of the incident plane wave. But, as the numerical aperture increases, the maximum value of the longitudinal component of the electric field in the focal plane becomes quite substantial, although it vanishes at the focal point itself.

An appropriately shaped focused spot is essential in many applications such as optical recording, photolithography, and microscopy. Furthermore, a field in focus with maximum electric component in a specific direction is important for manipulating single molecules and particles, and in materials processing [5–9]. The focused wave front can be tailored by setting a proper amplitude, phase, and polarization distributions in the pupil of the focusing lens. Nowadays it is possible to realize almost any complex transmission function in the pupil plane, using, for example, liquid-crystal-based devices [10–14].

In this paper, we maximize a specified component of the electric field in the focal point of a diffraction-limited lens. First we consider fields in free space or in homogeneous matter, without taking into account the way these fields are realized, in particular without considering the lens. We merely suppose that, with respect to a Cartesian coordinate system (x,y,z), the fields considered consist of plane waves propagating in the positive z direction and have wave vectors with angles with the positive z axis that do not exceed a specific maximum angle, i.e., the numerical aperture of the plane waves is restricted. The optimization problem is then to find the complex plane wave amplitudes such that, for a given direction in space and for given mean flow of electromagnetic power through a plane $z=$const, the amplitude at some point (chosen at the origin) of the electric field component that is parallel to the chosen direction is larger than that of any other field for the same numerical aperture and the same mean total power flow. We shall derive closed formulas for the plane wave amplitudes of the optimum field.

The solutions of the optimization problems for the field propagating in homogeneous space is rigorous results since they are derived from Maxwell's equations without any further assumptions. Next we will consider the realization of the optimum field using a diffraction-limited lens with the origin as the focal point. By using the vector diffraction theory of Ignatowksy and Richards and Wolf, closed expressions for the optimum pupil distributions will be derived, which after focusing give the optimum field component in the focal point of the lens. In contrast with the solution in terms of the plane wave expansion, the formulas for the optimum pupil fields are approximate since they are based on the vector diffraction theory which is an approximate theory that is valid for lenses of which the focal distance and the pupil radius are many wavelengths.

When one considers the focusing by a lens it is obvious that the plane wave expansion in image space has finite numerical aperture of that of the lens, $\mathrm{NA}=n\sin\alpha_{\max}$, where n is the refractive index in image space and $\alpha_{\max}$ is half the top angle of the cone with the top the focal point and the base the pupil. But also when one would consider only waves in free space without a focusing lens, there is a good reason to restrict the fields to finite numerical aperture, in that case in particular to $\mathrm{NA}=n$. In fact, when $\mathrm{NA}>n$ a part of the evanescent waves are taken into account in the expansion. One can then construct fields with a given power which have arbitrary large components. The evanescent waves do not contribute to the total power and hence one can increase their amplitudes by any desired amount to achieve arbitrarily high local fields. Stated differently, by constructing suitable time-harmonic source distributions that emit singular fields with finite power flow, one can achieve arbitrary large field components by approaching these source distributions. At small distances to the sources the evanescent waves of course play a major role.

Among the directions for the optimized electric field component, two are of particular interest, namely, the directions parallel and perpendicular to the optical z axis. These direc-

*h.p.urbach@tudelft.nl

tions are also called the longitudinal and transverse directions. The field with maximum longitudinal component has been discussed in [15], but without derivation. In this paper details of the derivation are provided and the optimization problem is generalized to arbitrary directions of the electric field vector.

As was announced in [15], the pupil field that when focused gives maximum longitudinal component, is radially polarized. This means that in all points of the lens pupil, the electric field is linearly polarized with the electric field pointing in the radial direction. Furthermore, the electric fields in all points of the pupil are in phase and the electric field amplitudes are rotationally symmetric. The amplitude of the electric pupil field vanishes at the center of the pupil and is a monotonically increasing function of the radial coordinate. The shape of this function depends on the numerical aperture.

It was noted by several authors [16–19] that when a radially polarized beam is focused, the distribution of the longitudinal component can be considerably narrower than the focused spot obtained by focusing a linearly polarized plane wave. With the development of a new generation of photoresists [20], it is possible to control the photosensitive material in such a way that it will react to only one of the polarization components of the electric field. Materials with molecules having fixed absorption dipole moments have been applied in [6] to be able to probe field components individually. When this component is the longitudinal component, a tighter spot can thus be obtained than with the classical Airy pattern.

Often the amplitude distribution of the radially polarized beam in the pupil plane is chosen to be a doughnut shape or a ring mask function [17]. But these distributions do not give the maximum possible longitudinal electric field component in focus for the given power and its amplitude as a function of the radial pupil coordinate differs from the optimum function derived in the present paper.

The other case of particular interest is the optimization of the transverse electric field vector. Since the optical system is assumed to be rotationally symmetric around the optical axis, we may choose this direction parallel to the x axis. The solution of the optimization problem is then the field for which the amplitude of the x component of the electric field in the focal point is maximum for the given numerical aperture and the given total power flow. We will show that the corresponding pupil field is linearly polarized with direction of polarization predominantly, although not exactly, parallel to the x axis. Therefore, the focused optimum field is similar to the vectorial Airy pattern of a focused linearly polarized plane wave, although it is *not* identical to it.

The paper is organized as follows. In Sec. II, we will formulate the optimization problem and we will prove that the optimization problem has one and only one solution. In Sec. III, we will apply the Lagrange multiplier rule to obtain closed formulas for the plane wave amplitudes of the optimum field and for the optimum field distributions near focus. In Sec. IV, we will study the optimum fields in the focal region, in particular their mean energy flow. Then, in Sec. V, we apply the vector diffraction theory of Ignatowsky and Richards and Wolf to derive the electric field distribution in the pupil of the lens that, when focused, yields the maximum field component in the focal region.

II. FORMULATION OF THE OPTIMIZATION PROBLEM FOR ARBITRARY ELECTRIC FIELD COMPONENT

We begin with some notations. Consider a time-harmonic electromagnetic field in a homogeneous unbounded medium with real refractive index n (i.e., the material does not absorb electromagnetic radiation of the given frequency),

$$\boldsymbol{\mathcal{E}}(\mathbf{r},t) = \mathrm{Re}[\mathbf{E}(\mathbf{r})e^{-i\omega t}], \tag{1}$$

$$\boldsymbol{\mathcal{H}}(\mathbf{r},t) = \mathrm{Re}[\mathbf{H}(\mathbf{r})e^{-i\omega t}], \tag{2}$$

where $\omega > 0$. As stated in the Introduction, the lens is first not considered in the optimization problem. It is merely assumed that, with respect to the Cartesian coordinate system (x,y,z) with unit vectors $\hat{\mathbf{x}}$, $\hat{\mathbf{y}}$, and $\hat{\mathbf{z}}$, the electromagnetic field (1) and (2) has numerical aperture $\mathrm{NA} \leqslant n$ and that the plane wave vectors have positive z component,

$$\mathbf{E}(\mathbf{r}) = \frac{1}{4\pi^2}\int\int_{\sqrt{k_x^2+k_y^2}\leqslant k_0 n\ \sin\alpha_{\max}} \mathbf{A}(k_x,k_y)e^{i\mathbf{k}\cdot\mathbf{r}}dk_x dk_y, \tag{3}$$

$$\mathbf{H}(\mathbf{r}) = \frac{1}{4\pi^2}\frac{1}{\omega\mu_0}\int\int_{\sqrt{k_x^2+k_y^2}\leqslant k_0 n\ \sin\alpha_{\max}} \mathbf{k}\times\mathbf{A}(k_x,k_y) \times e^{i\mathbf{k}\cdot\mathbf{r}}dk_x dk_y, \tag{4}$$

where $\mathbf{k}=(k_x,k_y,k_z)$ with

$$k_z = (k_0^2 n^2 - k_x^2 - k_y^2)^{1/2}, \tag{5}$$

with $k_0=\omega\sqrt{\epsilon_0\mu_0}=2\pi/\lambda_0$, where λ_0 is the wavelength in vacuum, and where $\mathrm{NA}=n\sin\alpha_{\max}$ with $\alpha_{\max}$ the maximum angle that the wave vectors make with the positive z direction. If $\mathrm{NA}=n$ we have $\alpha_{\max}=\pi/2$ and the plane wave spectrum then consists of all homogeneous plane waves that propagate in the non-negative z direction (there are no evanescent waves in the expansion). When $\mathrm{NA}<n$, the cone of allowed wave vectors has top angle $\alpha_{\max}=\arcsin(\mathrm{NA}/n) < 90°$. Because the electric field is free of divergence we have that

$$\mathbf{A}\cdot\mathbf{k} = 0. \tag{6}$$

We shall use spherical coordinates in reciprocal $\mathbf{k}$ space,

$$\hat{\mathbf{k}} = \sin\alpha\cos\beta\hat{\mathbf{x}} + \sin\alpha\sin\beta\hat{\mathbf{y}} + \cos\alpha\hat{\mathbf{z}}, \tag{7}$$

$$\hat{\boldsymbol{\alpha}} = \cos\alpha\cos\beta\hat{\mathbf{x}} + \cos\alpha\sin\beta\hat{\mathbf{y}} - \sin\alpha\hat{\mathbf{z}}, \tag{8}$$

$$\hat{\boldsymbol{\beta}} = -\sin\beta\hat{\mathbf{x}} + \cos\beta\hat{\mathbf{y}}, \tag{9}$$

where $0\leqslant\alpha\leqslant\alpha_{\max}$ and $0\leqslant\beta<2\pi$ are the polar and azimuthal angles, respectively. Conversely, we have

$$\hat{\mathbf{x}} = \sin\alpha\cos\beta\hat{\mathbf{k}} + \cos\alpha\cos\beta\hat{\boldsymbol{\alpha}} - \sin\beta\hat{\boldsymbol{\beta}}, \tag{10}$$

$$\hat{\mathbf{y}} = \sin\alpha\sin\beta\hat{\mathbf{k}} + \cos\alpha\sin\beta\hat{\boldsymbol{\alpha}} + \cos\beta\hat{\boldsymbol{\beta}}, \tag{11}$$

$$\hat{\mathbf{z}} = \cos\alpha\hat{\mathbf{k}} - \sin\alpha\hat{\boldsymbol{\alpha}}. \tag{12}$$

Note that $\{\hat{\mathbf{k}}, \hat{\boldsymbol{\alpha}}, \hat{\boldsymbol{\beta}}\}$ is a positively oriented orthonormal basis,

$$\hat{\mathbf{k}} \times \hat{\boldsymbol{\alpha}} = \hat{\boldsymbol{\beta}}, \quad \hat{\boldsymbol{\alpha}} \times \hat{\boldsymbol{\beta}} = \hat{\mathbf{k}}, \quad \hat{\boldsymbol{\beta}} \times \hat{\mathbf{k}} = \hat{\boldsymbol{\alpha}}. \tag{13}$$

Furthermore, $\mathbf{k} = k_0 n\hat{\mathbf{k}}$ and the Jacobian of the transformation $(\alpha, \beta) \mapsto (k_x, k_y)$ is

$$\begin{pmatrix} \frac{\partial k_x}{\partial \alpha} & \frac{\partial k_x}{\partial \beta} \\ \frac{\partial k_y}{\partial \alpha} & \frac{\partial k_y}{\partial \beta} \end{pmatrix} = k_0 n \begin{pmatrix} \cos\alpha\cos\beta & -\sin\alpha\sin\beta \\ \cos\alpha\sin\beta & \sin\alpha\cos\beta \end{pmatrix}, \tag{14}$$

so that

$$dk_x dk_y = k_0^2 n^2 \cos\alpha \sin\alpha d\alpha d\beta. \tag{15}$$

Because of Eq. (6) we have

$$\mathbf{A}(\alpha, \beta) = A_\alpha(\alpha, \beta)\hat{\boldsymbol{\alpha}} + A_\beta(\alpha, \beta)\hat{\boldsymbol{\beta}}, \tag{16}$$

for some functions A_α and A_β. Then, using Eq. (13),

$$\mathbf{k} \times \mathbf{A} = k_0 n(-A_\beta\hat{\boldsymbol{\alpha}} + A_\alpha\hat{\boldsymbol{\beta}}). \tag{17}$$

The plane wave expansion can thus be written as

$$\mathbf{E}(\mathbf{r}) = \frac{n^2}{\lambda_0^2}\int_0^{\alpha_{\max}}\int_0^{2\pi}(A_\alpha\hat{\boldsymbol{\alpha}} + A_\beta\hat{\boldsymbol{\beta}})\cos\alpha\sin\alpha e^{i\mathbf{k}\cdot\mathbf{r}} d\alpha d\beta, \tag{18}$$

$$\mathbf{H}(\mathbf{r}) = \frac{n^3}{\lambda_0^2}\left(\frac{\epsilon_0}{\mu_0}\right)^{1/2}\int_0^{\alpha_{\max}}\int_0^{2\pi}(-A_\beta\hat{\boldsymbol{\alpha}} + A_\alpha\hat{\boldsymbol{\beta}})\cos\alpha\sin\alpha e^{i\mathbf{k}\cdot\mathbf{r}} d\alpha d\beta. \tag{19}$$

The $\hat{\boldsymbol{\alpha}}$ component is parallel to the plane through the wave vector and the z axis, whereas the $\hat{\boldsymbol{\beta}}$ component is perpendicular to this plane.

Let $\hat{\mathbf{v}} = v_x\hat{\mathbf{x}} + v_y\hat{\mathbf{y}} + v_z\hat{\mathbf{z}}$ be a real unit vector. We consider the projection of the electric field at the origin at time $t=0$ on the direction of $\hat{\mathbf{v}}$,

$$\mathbf{E}(\mathbf{0}) \cdot \hat{\mathbf{v}} = \frac{n^2}{\lambda_0^2}\int_0^{\alpha_{\max}}\int_0^{2\pi}[A_\alpha(\alpha, \beta)v_\alpha + A_\beta(\alpha, \beta)v_\beta]\cos\alpha\sin\alpha d\alpha d\beta, \tag{20}$$

where

$$v_\alpha = \hat{\mathbf{v}} \cdot \hat{\boldsymbol{\alpha}} = v_x\cos\alpha\cos\beta + v_y\cos\alpha\sin\beta - v_z\sin\alpha, \tag{21}$$

$$v_\beta = \hat{\mathbf{v}} \cdot \hat{\boldsymbol{\beta}} = -v_x\sin\beta + v_y\cos\beta. \tag{22}$$

We will consider $\mathbf{E}(\mathbf{0}) \cdot \hat{\mathbf{v}}$ as a (linear) functional of $\mathbf{A} = A_\alpha\hat{\boldsymbol{\alpha}} + A_\beta\hat{\boldsymbol{\beta}}$, which for brevity we will denote by $F(\mathbf{A})$. Hence,

$$F(\mathbf{A}) \overset{\text{def.}}{=} \frac{n^2}{\lambda_0^2}\int_0^{\alpha_{\max}}\int_0^{2\pi}[A_\alpha(\alpha, \beta)v_\alpha + A_\beta(\alpha, \beta)v_\beta]\cos\alpha\sin\alpha d\alpha d\beta. \tag{23}$$

Next, we calculate the total mean flow of power through a plane $z=$const. The total mean power flow is obtained by integrating the normal component of the vector $(1/2)\mathrm{Re}\,\mathbf{S}$ over the plane $z=$const, where $\mathbf{S} = \mathbf{E} \times \mathbf{H}^*$ is the complex Poynting vector. By using Plancherel's formula, the integral of $\mathrm{Re}\,\mathbf{S}$ over this plane can be written as an integral over k_x and k_y,

$$\begin{aligned}\int_{-\infty}^{\infty}\int_{-\infty}^{\infty}\frac{1}{2}\mathrm{Re}[\mathbf{S}(\mathbf{r})]dxdy &= \frac{1}{2}\mathrm{Re}\int_{-\infty}^{\infty}\int_{-\infty}^{\infty}\mathbf{E}(\mathbf{r}) \times \mathbf{H}(\mathbf{r})^* dxdy \\ &= \frac{1}{8\pi^2}\mathrm{Re}\int\int_{\sqrt{k_x^2+k_y^2}\le \mathrm{NA}k_0}\mathbf{A}(k_x, k_y)e^{ik_z z} \times \left[\frac{\mathbf{k}}{\omega\mu_0} \times \mathbf{A}(k_x, k_y)^*\right]e^{-ik_z z}dk_x dk_y \\ &= \frac{1}{8\pi^2}\frac{1}{\omega\mu_0}\int\int_{\sqrt{k_x^2+k_y^2}\le \mathrm{NA}k_0}|\mathbf{A}(k_x, k_y)|^2\mathbf{k}dk_x dk_y,\end{aligned} \tag{24}$$

where we used that $\mathbf{k}$ is real and $\mathbf{A}(k_x, k_y) \cdot \mathbf{k} = 0$. The total time-averaged flow of energy in the positive z direction through the plane $z=$const is given by the z component of Eq. (24),

$$\begin{aligned}\int_{-\infty}^{\infty}\int_{-\infty}^{\infty}\frac{1}{2}\mathrm{Re}[S_z(\mathbf{r})]dxdy &= \frac{1}{8\pi^2}\frac{1}{\omega\mu_0}\int\int_{\sqrt{k_x^2+k_y^2}\le \mathrm{NA}k_0}|\mathbf{A}(k_x, k_y)|^2 k_z dk_x dk_y \\ &= \frac{n^3}{2\lambda_0^2}\left(\frac{\epsilon_0}{\mu_0}\right)^{1/2}\int_0^{\alpha_{\max}}\int_0^{2\pi}[|A_\alpha(\alpha, \beta)|^2 + |A_\beta(\alpha, \beta)|^2]\cos^2\alpha\sin\alpha d\alpha d\beta.\end{aligned} \tag{25}$$

This is independent of the plane $z=$const, as should be in a medium without losses.

The quantity $F(\mathbf{A})=\mathbf{E}(0)\cdot\hat{\mathbf{v}}$ is the complex electric field component in the direction of $\hat{\mathbf{v}}$ at time $t=0$. Without restricting the generality we may assume that $F(\mathbf{A})$ is real. If it were not real, a time shift could be applied to make it real. Hence we may assume that

$$\mathrm{Im}[\mathbf{E}(0)\cdot\hat{\mathbf{v}}]=\int_0^{\alpha_{\max}}\int_0^{2\pi}\mathrm{Im}[A_\alpha(\alpha,\beta)v_\alpha + A_\beta(\alpha,\beta)v_\beta]\cos\alpha\sin\alpha d\alpha d\beta=0. \quad (26)$$

The optimization problem is to find the plane wave amplitudes $\mathbf{A}=A_\alpha\hat{\boldsymbol{\alpha}}+A_\beta\hat{\boldsymbol{\beta}}$ for which the electric field component at the origin $\mathbf{0}$ that is parallel to the direction of $\hat{\mathbf{v}}$ is larger than for any other field with the same mean power flow through a plane $z=$const and the same numerical aperture. To formulate this problem mathematically, we introduce the space $\mathcal{H}$ of plane wave amplitudes $\mathbf{A}=A_\alpha\hat{\boldsymbol{\alpha}}+A_\beta\hat{\boldsymbol{\beta}}$ which have finite mean flow of power through the planes $z=$const,

$$\mathcal{H}=\left\{\mathbf{A}=A_\alpha\hat{\boldsymbol{\alpha}}+A_\beta\hat{\boldsymbol{\beta}};\int_0^{\alpha_{\max}}\int_0^{2\pi}[|A_\alpha(\alpha,\beta)|^2 + |A_\beta(\alpha,\beta)|^2]\cos^2\alpha\sin\alpha d\alpha d\beta<\infty\right\}, \quad (27)$$

and we define $\mathcal{H}_0$ as the subspace of $\mathcal{H}$ consisting of all $\mathbf{A}$ which satisfy Eq. (26). Then $\mathcal{H}$ is a Hilbert space with scalar product

$$\langle\mathbf{A},\mathbf{B}\rangle_{\mathcal{H}}=\int_0^{\alpha_{\max}}\int_0^{2\pi}[A_\alpha(\alpha,\beta)B_\alpha(\alpha,\beta)^* + A_\beta(\alpha,\beta)B_\beta(\alpha,\beta)^*]\cos^2\alpha\sin\alpha d\alpha d\beta, \quad (28)$$

and $\mathcal{H}_0$ is a closed subspace of $\mathcal{H}$. Note that the constraint (26) means that $\mathrm{Im}(\mathbf{A})$ is perpendicular to the vector field $\hat{\mathbf{v}}/\cos\alpha$ in the space $\mathcal{H}$, i.e., $\mathrm{Im}(\mathbf{A})$ is perpendicular to $\hat{\mathbf{v}}/\cos\alpha$ in the sense of scalar product (28).

Define the quadratic functional

$$P(\mathbf{A})\overset{\text{def.}}{=}\frac{n^3}{2\lambda_0^2}\left(\frac{\epsilon_0}{\mu_0}\right)^{1/2}\int_0^{\alpha_{\max}}\int_0^{2\pi}[|A_\alpha(\alpha,\beta)|^2 + |A_\beta(\alpha,\beta)|^2]\cos^2\alpha\sin\alpha d\alpha d\beta, \quad (29)$$

which is the mean power flowing through a plane $z=$const for fields with plane wave amplitudes $\mathbf{A}=A_\alpha\hat{\boldsymbol{\alpha}}+A_\beta\hat{\boldsymbol{\beta}}$. Then the optimization problem is to find, for given $P_0>0$, the solution of

$$(*)\ \max_{\mathbf{A}\in\mathcal{H}_0}F(\mathbf{A}),\quad \text{under the constraint } P(\mathbf{A})\leqslant P_0.$$

For any solution of problem $(*)$ the equality $P(\mathbf{A})=P_0$ holds, because otherwise $\mathbf{A}$ could be multiplied by the number $[P_0/P(\mathbf{A})]^{1/2}>1$ and this would increase the value of F without violating the constraint on the energy. Hence it does not matter whether we impose the equality constraint $P(\mathbf{A})=P_0$ or the inequality constraint $P(\mathbf{A})\leqslant P_0$ on the mean flow of energy.

It is not completely obvious that problem $(*)$ has a unique solution since it is posed in a linear space $\mathcal{H}_0$ of infinite dimension. However, there is a functional analytic theorem which states that a continuous real linear functional attains its supremum on a sphere in a Hilbert space and that the solution is unique [21]. Since the functional F is linear, real and continuous with respect to the norm on $\mathcal{H}$, and since the feasible set of problem $(*)$ is a sphere in $\mathcal{H}_0$, this theorem applies to our problem. Hence the optimization problem has a unique solution. In the next section we shall compute the solution.

III. OPTIMUM PLANE WAVE AMPLITUDES

Since F is a linear functional, the Fréchet derivative of F at $\mathbf{A}$ in the direction of $\mathbf{B}$ is simply $F(\mathbf{B})$, i.e.,

$$\delta F(\mathbf{A})(\mathbf{B})=F(\mathbf{B})=\frac{n^2}{\lambda_0^2}\int_0^{\alpha_{\max}}\int_0^{2\pi}[B_\alpha(\alpha,\beta)v_\alpha + B_\beta(\alpha,\beta)v_\beta]\cos\alpha\sin\alpha d\alpha d\beta. \quad (30)$$

The Fréchet derivative of the quadratic functional $P(\mathbf{A})$ is

$$\delta P(A_\alpha)(B_\alpha)=\frac{n^3}{\lambda_0^2}\left(\frac{\epsilon_0}{\mu_0}\right)^{1/2}\mathrm{Re}\int_0^{\alpha_{\max}}\int_0^{2\pi}[A_\alpha(\alpha,\beta)B_\alpha(\alpha,\beta)^* + A_\beta(\alpha)B_\beta(\alpha,\beta)^*]\cos^2\alpha\sin\alpha d\alpha d\beta. \quad (31)$$

According to the Lagrange multiplier rule for inequality constraints (also known as Kuhn-Tucker's theorem) [22], there exists a Lagrange multiplier $\Lambda\geqslant 0$ such that, if $\mathbf{A}$ is the optimum field, we have

$$\delta F(\mathbf{A})(\mathbf{B})-\Lambda\delta P(\mathbf{A})(\mathbf{B})=0\quad \text{for all } \mathbf{B} \text{ in } \mathcal{H}_0, \quad (32)$$

and

$$\Lambda[P(\mathbf{A})-P_0]=0. \quad (33)$$

In the previous section we have shown that $P(\mathbf{A})=P_0$, therefore the last equation does not give new information. By substituting (30) and (31) into the Lagrange multiplier rule, we obtain

$$\frac{n^2}{\lambda_0^2}\int_0^{\alpha_{\max}}\int_0^{2\pi}[B_\alpha(\alpha,\beta)v_\alpha+B_\beta(\alpha,\beta)v_\beta]\cos\alpha\sin\alpha d\alpha d\beta - \Lambda\frac{n^3}{\lambda_0^2}\left(\frac{\epsilon_0}{\mu_0}\right)^{1/2}\mathrm{Re}\int_0^{\alpha_{\max}}\int_0^{2\pi}[A_\alpha(\alpha,\beta)B_\alpha(\alpha,\beta)^* + A_\beta(\alpha)B_\beta(\alpha,\beta)^*]\cos^2\alpha\sin\alpha d\alpha d\beta = 0,\quad \text{for all } \mathbf{B} \text{ in } \mathcal{H}_0. \quad (34)$$

Because $\mathbf{B}$ satisfies Eq. (26), it follows that in the first integral we may replace B_α and B_β by B_α^* and B_β^*, respectively. Hence,

$$\mathrm{Re}\int_0^{\alpha_{\max}}\int_0^{2\pi}\left\{\left[\frac{v_\alpha}{\cos\alpha}-\Lambda n\left(\frac{\epsilon_0}{\mu_0}\right)^{1/2}A_\alpha\right]B_\alpha^* + \left[\frac{v_\beta}{\cos\alpha}-\Lambda n\left(\frac{\epsilon_0}{\mu_0}\right)^{1/2}A_\beta\right]B_\beta^*\right\}\cos^2\alpha\sin\alpha d\alpha d\beta = 0, \quad \text{for all } \mathbf{B} \text{ in } \mathcal{H}_0. \tag{35}$$

This is equivalent to

$$\int_0^{\alpha_{\max}}\int_0^{2\pi}\left\{\left[\frac{v_\alpha}{\cos\alpha}-\Lambda n\left(\frac{\epsilon_0}{\mu_0}\right)^{1/2}\mathrm{Re}(A_\alpha)\right]\mathrm{Re}(B_\alpha) - \Lambda n\left(\frac{\epsilon_0}{\mu_0}\right)^{1/2}\mathrm{Im}(A_\alpha)\mathrm{Im}(B_\alpha) + \left[\frac{v_\beta}{\cos\alpha}-\Lambda n\left(\frac{\epsilon_0}{\mu_0}\right)^{1/2}\mathrm{Re}(A_\beta)\right]\mathrm{Re}(B_\beta) - \Lambda n\left(\frac{\epsilon_0}{\mu_0}\right)^{1/2}\mathrm{Im}(A_\beta)\mathrm{Im}(B_\beta)\right\}\cos^2\alpha\sin\alpha d\alpha d\beta = 0, \tag{36}$$

for all $\mathbf{B}$ in $\mathcal{H}_0$, i.e., for all $\mathbf{B}$ for which

$$\int_0^{\alpha_{\max}}\int_0^{2\pi}[\mathrm{Im}(B_\alpha)v_\alpha+\mathrm{Im}(B_\beta)v_\beta]\cos^2\alpha\sin\alpha d\alpha d\beta = 0. \tag{37}$$

Choose first B_α and B_β real. Then Eq. (37) is obviously satisfied and Eq. (36) implies

$$\mathrm{Re}(A_\alpha) = \frac{1}{\Lambda n}\left(\frac{\mu_0}{\epsilon_0}\right)^{1/2}\frac{v_\alpha}{\cos\alpha}, \tag{38}$$

$$\mathrm{Re}(A_\beta) = \frac{1}{\Lambda n}\left(\frac{\mu_0}{\epsilon_0}\right)^{1/2}\frac{v_\beta}{\cos\alpha}. \tag{39}$$

By substituting this in Eq. (36) it follows that

$$\int_0^{\alpha_{\max}}\int_0^{2\pi}[\mathrm{Im}(A_\alpha)\mathrm{Im}(B_\alpha) + \mathrm{Im}(A_\beta)\mathrm{Im}(B_\beta)]\cos^2\alpha\sin\alpha\, d\alpha\, d\beta = 0, \tag{40}$$

for all B_α, B_β that satisfy Eq. (37). This can be stated alternatively by saying that if $\mathbf{B}=B_\alpha\hat{\boldsymbol{\alpha}}+B_\beta\hat{\boldsymbol{\beta}}$ is perpendicular to $(v_\alpha/\cos\alpha)\hat{\boldsymbol{\alpha}}+(v_\beta/\cos\alpha)\hat{\boldsymbol{\beta}}$, then $\mathbf{B}$ is perpendicular to $\mathrm{Im}(A_\alpha)\hat{\boldsymbol{\alpha}}+\mathrm{Im}(A_\beta)\hat{\boldsymbol{\beta}}$ [perpendicular means here of course with respect to scalar product (28)]. We conclude that $\mathrm{Im}(A_\alpha)\hat{\boldsymbol{\alpha}}+\mathrm{Im}(A_\beta)\hat{\boldsymbol{\beta}}$ is proportional to $(v_\alpha/\cos\alpha)\hat{\boldsymbol{\alpha}}+(v_\beta/\cos\alpha)\hat{\boldsymbol{\beta}}$,

$$\mathrm{Im}(A_\alpha) = C\frac{v_\alpha}{\cos\alpha}, \tag{41}$$

$$\mathrm{Im}(A_\beta) = C\frac{v_\beta}{\cos\alpha}, \tag{42}$$

for some constant C. We shall now show that $C=0$. By substitution of Eqs. (41) and (42) into Eq. (26) we obtain

$$C\int_0^{\alpha_{\max}}\int_0^{2\pi}(v_\alpha^2+v_\beta^2)\cos\alpha\sin\alpha d\alpha d\beta = 0. \tag{43}$$

If $C\neq 0$, then we must have

$$v_\alpha = v_\beta = 0, \text{ for all } \alpha,\beta \text{ with } 0\leqslant\alpha\leqslant\alpha_{\max}, \quad 0\leqslant\beta\leqslant 2\pi. \tag{44}$$

Use the expressions (21) and (22) for v_α and v_β in terms of the Cartesian components v_x, v_y, and v_z. It is then easily seen that Eq. (44) implies $v_x=v_y=v_z=0$. This contradicts the assumption that $\mathbf{v}$ is a unit vector. Hence $C=0$.

We thus conclude that the plane wave amplitudes of the optimum field are given by

$$A_\alpha = \frac{1}{\Lambda n}\left(\frac{\mu_0}{\epsilon_0}\right)^{1/2}\frac{v_\alpha}{\cos\alpha}, \tag{45}$$

$$A_\beta = \frac{1}{\Lambda n}\left(\frac{\mu_0}{\epsilon_0}\right)^{1/2}\frac{v_\beta}{\cos\alpha}. \tag{46}$$

The Lagrange multiplier Λ can be determined by substituting Eqs. (45) and (46) into $P(\mathbf{A})=P_0$ and then using Eqs. (21) and (22). We find

$$P(\mathbf{A}) = \frac{n}{2\Lambda^2\lambda_0^2}\left(\frac{\mu_0}{\epsilon_0}\right)^{1/2}\int_0^{\alpha_{\max}}\int_0^{2\pi}(v_\alpha^2+v_\beta^2)\sin\alpha d\alpha d\beta \tag{47}$$

$$= \frac{n}{2\Lambda^2\lambda_0^2}\left(\frac{\mu_0}{\epsilon_0}\right)^{1/2}\left\{v_x^2\int_0^{\alpha_{\max}}\int_0^{2\pi}(\cos^2\alpha\cos^2\beta+\sin^2\beta)\sin\alpha d\alpha d\beta + v_y^2\int_0^{\alpha_{\max}}\int_0^{2\pi}(\cos^2\alpha\sin^2\beta+\cos^2\beta)\sin\alpha d\alpha d\beta + v_z^2\int_0^{\alpha_{\max}}\int_0^{2\pi}\sin^3\alpha d\alpha d\beta - 2v_xv_y\int_0^{\alpha_{\max}}\int_0^{2\pi}\sin^3\alpha\cos\beta\sin\beta d\alpha d\beta - 2v_xv_z\int_0^{\alpha_{\max}}\int_0^{2\pi}\cos\alpha\sin^2\alpha\cos\beta d\alpha d\beta$$

$$
\begin{aligned}
&- 2v_y v_z \int_0^{\alpha_{\max}} \int_0^{2\pi} \cos\alpha \sin^2\alpha \sin\beta d\alpha d\beta \Bigg\} \\
&= \frac{\pi n}{2\Lambda^2 \lambda_0^2} \left(\frac{\mu_0}{\epsilon_0}\right)^{1/2} \left[\left(\frac{4}{3} - \cos\alpha_{\max} - \frac{1}{3}\cos^3\alpha_{\max}\right)(v_x^2 + v_y^2) + \left(\frac{4}{3} - 2\cos\alpha_{\max} + \frac{2}{3}\cos^3\alpha_{\max}\right) v_z^2 \right] \\
&= \frac{\pi n}{2\Lambda^2 \lambda_0^2} \left(\frac{\mu_0}{\epsilon_0}\right)^{1/2} \left[\frac{4}{3} - \cos\alpha_{\max} - \frac{1}{3}\cos^3\alpha_{\max} - \sin^2\alpha_{\max}\cos\alpha_{\max} v_z^2 \right]. \qquad (48)
\end{aligned}
$$

It follows from $P(\mathbf{A}) = P_0$ and $\Lambda \geqslant 0$ that

$$
\Lambda = \sqrt{\frac{\pi}{2}} \frac{n^{1/2}}{P_0^{1/2}\lambda_0} \left(\frac{\mu_0}{\epsilon_0}\right)^{1/4} \left[\frac{4}{3} - \cos\alpha_{\max} - \frac{1}{3}\cos^3\alpha_{\max} - \sin^2\alpha_{\max}\cos\alpha_{\max} v_z^2 \right]^{1/2}. \qquad (49)
$$

Herewith the derivation of the plane waves amplitudes of the optimum field is complete.

The maximum of the field component at the origin, i.e., of F, is

$$
\begin{aligned}
F_{\max} = F(\mathbf{A}) &= \frac{n^2}{\lambda_0^2} \int_0^{\alpha_{\max}} \int_0^{2\pi} [A_\alpha(\alpha,\beta) v_\alpha + A_\beta(\alpha,\beta) v_\beta] \cos\alpha \sin\alpha d\alpha d\beta \\
&= \frac{1}{\Lambda} \frac{n}{\lambda_0^2} \left(\frac{\mu_0}{\epsilon_0}\right)^{1/2} \int_0^{\alpha_{\max}} \int_0^{2\pi} (v_\alpha^2 + v_\beta^2) \sin\alpha d\alpha d\beta \\
&= 2\Lambda P_0 \\
&= \sqrt{2\pi} P_0^{1/2} \frac{n^{1/2}}{\lambda_0} \left(\frac{\mu_0}{\epsilon_0}\right)^{1/4} \left[\frac{4}{3} - \cos\alpha_{\max} - \frac{1}{3}\cos^3\alpha_{\max} - \sin^2\alpha_{\max}\cos\alpha_{\max} v_z^2 \right]^{1/2}, \qquad (50)
\end{aligned}
$$

where we used Eqs. (47) and (49).

IV. THE OPTIMUM ELECTROMAGNETIC FIELD

The electric field amplitudes of the plane waves of the optimum field are given by

$$
\begin{aligned}
\mathbf{A}(\alpha,\beta) &= A_\alpha(\alpha,\beta)\hat{\boldsymbol{\alpha}} + A_\beta(\alpha,\beta)\hat{\boldsymbol{\beta}} \\
&= \frac{1}{\Lambda n}\left(\frac{\mu_0}{\epsilon_0}\right)^{1/2} (v_\alpha \hat{\boldsymbol{\alpha}} + v_\beta \hat{\boldsymbol{\beta}}) \frac{1}{\cos\alpha} = \frac{1}{\Lambda n}\left(\frac{\mu_0}{\epsilon_0}\right)^{1/2} \left[\left(\cos\beta\hat{\boldsymbol{\alpha}} - \frac{\sin\beta}{\cos\alpha}\hat{\boldsymbol{\beta}}\right) v_x + \left(\sin\beta\hat{\boldsymbol{\alpha}} + \frac{\cos\beta}{\cos\alpha}\hat{\boldsymbol{\beta}}\right) v_y - \tan\alpha\hat{\boldsymbol{\alpha}} v_z \right] \\
&= \frac{1}{\Lambda n}\left(\frac{\mu_0}{\epsilon_0}\right)^{1/2} \left\{ \left[\left(\cos\alpha\cos^2\beta + \frac{\sin^2\beta}{\cos\alpha}\right)\hat{\mathbf{x}} - \frac{\sin^2\alpha}{\cos\alpha}\cos\beta\sin\beta\hat{\mathbf{y}} - \sin\alpha\cos\beta\hat{\mathbf{z}} \right] v_x \right. \\
&\quad + \left[-\frac{\sin^2\alpha}{\cos\alpha}\cos\beta\sin\beta\hat{\mathbf{x}} + \left(\cos\alpha\sin^2\beta + \frac{\cos^2\beta}{\cos\alpha}\right)\hat{\mathbf{y}} - \sin\alpha\sin\beta\hat{\mathbf{z}} \right] v_y \\
&\quad \left. + \left[-\sin\alpha\cos\beta\hat{\mathbf{x}} - \sin\alpha\sin\beta\hat{\mathbf{y}} + \frac{\sin^2\alpha}{\cos\alpha}\hat{\mathbf{z}} \right] v_z \right\}. \qquad (51)
\end{aligned}
$$

If we write the right-hand side of Eq. (51) as the product of a matrix and the vector $\mathbf{v}$ on the Cartesian basis $\hat{\mathbf{x}}$, $\hat{\mathbf{y}}$, $\hat{\mathbf{z}}$, we obtain

$$
\mathbf{A}(\alpha,\beta) = \frac{1}{\Lambda n}\left(\frac{\mu_0}{\epsilon_0}\right)^{1/2} \begin{pmatrix} \cos\alpha\cos^2\beta + \frac{\sin^2\beta}{\cos\alpha} & -\frac{\sin^2\alpha}{\cos\alpha}\cos\beta\sin\beta & -\sin\alpha\cos\beta \\ -\frac{\sin^2\alpha}{\cos\alpha}\cos\beta\sin\beta & \cos\alpha\sin^2\beta + \frac{\cos^2\beta}{\cos\alpha} & -\sin\alpha\sin\beta \\ -\sin\alpha\cos\beta & -\sin\alpha\sin\beta & \frac{\sin^2\alpha}{\cos\alpha} \end{pmatrix} \begin{pmatrix} v_x \\ v_y \\ v_z \end{pmatrix}.
$$

We shall use cylindrical coordinates ϱ, φ, z for the point of observation $\mathbf{r}$. There holds

$$\varrho = r \sin \varphi, \quad z = r \cos \varphi, \tag{52}$$

and the unit vectors $\hat{\boldsymbol{\varphi}}$, $\hat{\boldsymbol{\varrho}}$ are defined by

$$\hat{\boldsymbol{\varrho}} = \cos \varphi \hat{\mathbf{x}} + \sin \varphi \hat{\mathbf{y}}, \quad \hat{\boldsymbol{\varphi}} = -\sin \varphi \hat{\mathbf{x}} + \cos \varphi \hat{\mathbf{y}}. \tag{53}$$

Then

$$\begin{aligned}\mathbf{k} \cdot \mathbf{r} &= k_0 n(x \sin \alpha \cos \beta + y \sin \alpha \sin \beta + z \cos \alpha) = k_0 n(\varrho \cos \varphi \sin \alpha \cos \beta + \varrho \sin \varphi \sin \alpha \sin \beta + z \cos \alpha) \\ &= k_0 n[\varrho \sin \alpha \cos(\varphi - \beta) + z \cos \alpha] = k_0 n \varrho \sin \alpha \cos(\varphi - \beta) + k_0 n z \cos \alpha.\end{aligned} \tag{54}$$

The optimum electric field in a point $\mathbf{r}$ with cylindrical coordinates ϱ, φ, z is then

$$\begin{aligned}\mathbf{E}(\varrho, \varphi, z) &= \frac{n^2}{\lambda_0^2} \int_0^{\alpha_{\max}} \int_0^{2\pi} [A_\alpha(\alpha, \beta)\hat{\boldsymbol{\alpha}} + A_\beta(\alpha, \beta)\hat{\boldsymbol{\beta}}] e^{i\mathbf{k}\cdot\mathbf{r}} \sin \alpha \cos \alpha d\alpha d\beta \\ &= \frac{n}{\Lambda \lambda_0^2} \left(\frac{\mu_0}{\epsilon_0}\right)^{1/2} \int_0^{\alpha_{\max}} \sin \alpha e^{ik_0 n z \cos \alpha} d\alpha \int_0^{2\pi} \begin{pmatrix} 1 - \sin^2 \alpha \cos^2 \beta & -\sin^2 \alpha \cos \beta \sin \beta & -\cos \alpha \sin \alpha \cos \beta \\ -\sin^2 \alpha \cos \beta \sin \beta & 1 - \sin^2 \alpha \sin^2 \beta & -\cos \alpha \sin \alpha \sin \beta \\ -\cos \alpha \sin \alpha \cos \beta & -\cos \alpha \sin \alpha \sin \beta & \sin^2 \alpha \end{pmatrix} \\ &\times \begin{pmatrix} v_x \\ v_y \\ v_z \end{pmatrix} e^{ik_0 n \varrho \sin \alpha \cos(\beta - \varphi)} d\beta.\end{aligned} \tag{55}$$

Furthermore, the magnetic field amplitudes of the plane waves are (19)

$$\begin{aligned}-A_\beta(\alpha, \beta)\hat{\boldsymbol{\alpha}} + A_\alpha(\alpha, \beta)\hat{\boldsymbol{\beta}} &= \frac{1}{\Lambda n} \left(\frac{\mu_0}{\epsilon_0}\right)^{1/2} (-v_\beta \hat{\boldsymbol{\alpha}} + v_\alpha \hat{\boldsymbol{\beta}}) \frac{1}{\cos \alpha} \\ &= \frac{1}{\Lambda n} \left(\frac{\mu_0}{\epsilon_0}\right)^{1/2} \left[\left(-\frac{\sin \beta}{\cos \alpha} \hat{\boldsymbol{\alpha}} + \cos \beta \hat{\boldsymbol{\beta}} \right) v_x + \left(\frac{\cos \beta}{\cos \alpha} \hat{\boldsymbol{\alpha}} + \sin \beta \hat{\boldsymbol{\beta}} \right) v_y - \tan \alpha \hat{\boldsymbol{\beta}} v_z \right] \\ &= \frac{1}{\Lambda n} \left(\frac{\mu_0}{\epsilon_0}\right)^{1/2} \{[-2 \cos \beta \sin \beta \hat{\mathbf{x}} + (\cos^2 \beta - \sin^2 \beta)\hat{\mathbf{y}} + \tan \alpha \sin \beta \hat{\mathbf{z}}] v_x \\ &+ [(\cos^2 \beta - \sin^2 \beta)\hat{\mathbf{x}} + 2 \cos \beta \sin \beta \hat{\mathbf{y}} - \tan \alpha \cos \beta \hat{\mathbf{z}}] v_y + (\sin \beta \hat{\mathbf{x}} - \cos \beta \hat{\mathbf{y}}) \tan \alpha v_z \}.\end{aligned} \tag{56}$$

Hence, on the Cartesian basis

$$-A_\beta(\alpha, \beta)\hat{\boldsymbol{\alpha}} + A_\alpha(\alpha, \beta)\hat{\boldsymbol{\beta}} = \frac{1}{\Lambda n} \left(\frac{\mu_0}{\epsilon_0}\right)^{1/2} \begin{pmatrix} -2 \cos \beta \sin \beta & \cos^2 \beta - \sin^2 \beta & \tan \alpha \sin \beta \\ \cos^2 \beta - \sin^2 \beta & 2 \cos \beta \sin \beta & -\tan \alpha \cos \beta \\ \tan \alpha \sin \beta & -\tan \alpha \cos \beta & 0 \end{pmatrix} \begin{pmatrix} v_x \\ v_y \\ v_z \end{pmatrix}. \tag{57}$$

The optimum magnetic field is thus

$$\begin{aligned}\mathbf{H}(\varrho, \varphi, z) &= \frac{n^3}{\Lambda \lambda_0^2} \left(\frac{\epsilon_0}{\mu_0}\right)^{1/2} \int_0^{\alpha_{\max}} \int_0^{2\pi} [-A_\beta(\alpha, \beta)\hat{\boldsymbol{\alpha}} + A_\alpha(\alpha, \beta)\hat{\boldsymbol{\beta}}] e^{i\mathbf{k}\cdot\mathbf{r}} \sin \alpha \cos \alpha d\alpha d\beta \\ &= \frac{n^2}{\Lambda \lambda_0^2} \int_0^{\alpha_{\max}} \sin \alpha e^{ik_0 n z \cos \alpha} d\alpha \int_0^{2\pi} \begin{pmatrix} -\cos \alpha \sin(2\beta) & \cos \alpha \cos(2\beta) & \sin \alpha \sin \beta \\ \cos \alpha \cos(2\beta) & \cos \alpha \sin(2\beta) & -\sin \alpha \cos \beta \\ \sin \alpha \sin \beta & -\sin \alpha \cos \beta & 0 \end{pmatrix} \begin{pmatrix} v_x \\ v_y \\ v_z \end{pmatrix} e^{ik_0 n \varrho \sin \alpha \cos(\beta - \varphi)} d\beta.\end{aligned} \tag{58}$$

The integrals over β can be computed with the following formulas [23]:

$$\int_0^{2\pi} e^{i\zeta \cos(\beta - \varphi)} \cos(m\beta) d\beta = 2\pi i^m J_m(\zeta) \cos(m\varphi), \tag{59}$$

$$\int_0^{2\pi} e^{i\zeta \cos(\beta - \varphi)} \sin(m\beta) d\beta = 2\pi i^m J_m(\zeta) \sin(m\varphi), \tag{60}$$

for $m = 0, 1, 2, \ldots$. Hence,

$$\int_0^{2\pi} e^{i\zeta\cos(\beta-\varphi)}\cos^2\beta d\beta = \pi[J_0(\zeta) - J_2(\zeta)\cos(2\varphi)], \tag{61}$$

$$\int_0^{2\pi} e^{i\zeta\cos(\beta-\varphi)}\sin^2\beta d\beta = \pi[J_0(\zeta) + J_2(\zeta)\cos(2\varphi)], \tag{62}$$

$$\int_0^{2\pi} e^{i\zeta\cos(\beta-\varphi)}\cos\beta\sin\beta d\beta = -\pi J_2(\zeta)\sin(2\varphi). \tag{63}$$

By using the notation

$$g_l^{\nu,\mu}(\varrho,z) = \int_0^{\alpha_{\max}} e^{ik_0 nz\cos\alpha}\cos^\nu\alpha\sin^\mu\alpha J_l(k_0 n\varrho\sin\alpha)d\alpha, \tag{64}$$

the electric and magnetic fields can be expressed on the Cartesian basis as

$$\mathbf{E}(\varrho,\varphi,z) = \pi\frac{n}{\Lambda\lambda_0^2}\left(\frac{\mu_0}{\epsilon_0}\right)^{1/2}\left\{\begin{pmatrix} g_0^{0,1}(\varrho,z)+g_0^{2,1}(\varrho,z) & 0 & 0 \\ 0 & g_0^{0,1}(\varrho,z)+g_0^{2,1}(\varrho,z) & 0 \\ 0 & 0 & 2g_0^{0,3}(\varrho,z)\end{pmatrix}\right.$$
$$\left.+\begin{pmatrix} g_2^{0,3}(\varrho,z)\cos(2\varphi) & g_2^{0,3}(\varrho,z)\sin(2\varphi) & -2ig_1^{1,2}(\varrho,z)\cos\varphi \\ g_2^{0,3}(\varrho,z)\sin(2\varphi) & -g_2^{0,3}(\varrho,z)\cos(2\varphi) & -2ig_1^{1,2}(\varrho,z)\sin\varphi \\ -2ig_1^{1,2}(\varrho,z)\cos\varphi & -2ig_1^{1,2}(\varrho,z)\sin\varphi & 0\end{pmatrix}\right\}\begin{pmatrix}v_x\\v_y\\v_z\end{pmatrix}, \tag{65}$$

$$\mathbf{H}(\varrho,\varphi,z) = \frac{2\pi n^2}{\Lambda\lambda_0^2}\begin{pmatrix} g_2^{1,1}(\varrho,z)\sin(2\varphi) & -g_2^{1,1}(\varrho,z)\cos(2\varphi) & ig_1^{0,2}(\varrho,z)\sin\varphi \\ -g_2^{1,1}(\varrho,z)\cos(2\varphi) & -g_2^{1,1}(\varrho,z)\sin(2\varphi) & -ig_1^{0,2}(\varrho,z)\cos\varphi \\ ig_1^{0,2}(\varrho,z)\sin\varphi & -ig_1^{0,2}(\varrho,z)\cos\varphi & 0\end{pmatrix}\begin{pmatrix}v_x\\v_y\\v_z\end{pmatrix}. \tag{66}$$

Alternative concise expressions are obtained when the electric field, the magnetic field and the vector $\mathbf{v}$ are all written on the local cylindrical unit basis $\{\hat{\boldsymbol{\varrho}},\hat{\boldsymbol{\varphi}},\hat{\mathbf{z}}\}$ (attached to the point of observation $\mathbf{r}=\varrho\hat{\boldsymbol{\varrho}}+z\hat{\mathbf{z}}$),

$$\mathbf{E}(\varrho,\varphi,z) = \frac{\pi n}{\Lambda\lambda_0^2}\left(\frac{\mu_0}{\epsilon_0}\right)^{1/2}(\{[g_0^{0,1}(\varrho,z)+g_0^{2,1}(\varrho,z)+g_2^{0,3}(\varrho,z)]$$
$$\times(v_x\cos\varphi+v_y\sin\varphi)-2ig_1^{1,2}(\varrho,z)v_z\}\hat{\boldsymbol{\varrho}}$$
$$+[g_0^{0,1}(\varrho,z)+g_0^{2,1}(\varrho,z)-g_2^{0,3}(\varrho,z)](-v_x\sin\varphi$$
$$+v_y\cos\varphi)\hat{\boldsymbol{\varphi}}+[-2ig_1^{1,2}(\varrho,z)(v_x\cos\varphi+v_y\sin\varphi)$$
$$+2g_0^{0,3}(\varrho,z)v_z]\hat{\mathbf{z}}) \tag{67}$$

$$=\frac{\pi n}{\Lambda\lambda_0^2}\left(\frac{\mu_0}{\epsilon_0}\right)^{1/2}(\{[g_0^{0,1}(\varrho,z)+g_0^{2,1}(\varrho,z)$$
$$+g_2^{0,3}(\varrho,z)]v_\varrho-2ig_1^{1,2}(\varrho,z)v_z\}\hat{\boldsymbol{\varrho}}+[g_0^{0,1}(\varrho,z)$$
$$+g_0^{2,1}(\varrho,z)-g_2^{0,3}(\varrho,z)]v_\varphi\hat{\boldsymbol{\varphi}}+[-2ig_1^{1,2}(\varrho,z)v_\varrho$$
$$+2g_0^{0,3}(\varrho,z)v_z]\hat{\mathbf{z}}), \tag{68}$$

$$\mathbf{H}(\varrho,\varphi,z) = -\frac{2\pi n^2}{\Lambda\lambda_0^2}\{g_2^{1,1}(\varrho,z)(-v_x\sin\varphi+v_y\cos\varphi)\hat{\boldsymbol{\varrho}}$$
$$+[g_2^{1,1}(\varrho,z)(v_x\cos\varphi+v_y\sin\varphi)+ig_1^{0,2}(\varrho,z)v_z]\hat{\boldsymbol{\varphi}}$$
$$+ig_1^{0,2}(\varrho,z)(-v_x\sin\varphi+v_y\cos\varphi)\hat{\mathbf{z}}\} \tag{69}$$

$$=-\frac{2\pi n^2}{\Lambda\lambda_0^2}\{g_2^{1,1}(\varrho,z)v_\varphi\hat{\boldsymbol{\varrho}}+[g_2^{1,1}(\varrho,z)v_\varrho$$
$$+ig_1^{0,2}(\varrho,z)v_z]\hat{\boldsymbol{\varphi}}+ig_1^{0,2}(\varrho,z)v_\varphi\hat{\mathbf{z}}\}. \tag{70}$$

The time averaged Poynting vector of the optimum field is

$$\mathrm{Re}\,\mathbf{S}(\varrho,\varphi,z) = \frac{1}{2}\mathrm{Re}[\mathbf{E}(\varrho,\varphi,z)\times\mathbf{H}(\varrho,\varphi,z)^*]$$
$$=\frac{1}{2}\mathrm{Re}\{[E_\varphi(\varrho,\varphi,z)H_z(\varrho,\varphi,z)^*$$
$$-E_z(\varrho,\varphi,z)H_\varphi(\varrho,\varphi,z)^*]\hat{\boldsymbol{\varrho}}$$
$$+[E_z(\varrho,\varphi,z)H_\varrho(\varrho,\varphi,z)^*$$
$$-E_\varrho(\varrho,\varphi,z)H_z(\varrho,\varphi,z)^*]\hat{\boldsymbol{\varphi}}$$
$$+[E_\varrho(\varrho,\varphi,z)H_\varphi(\varrho,\varphi,z)^*$$

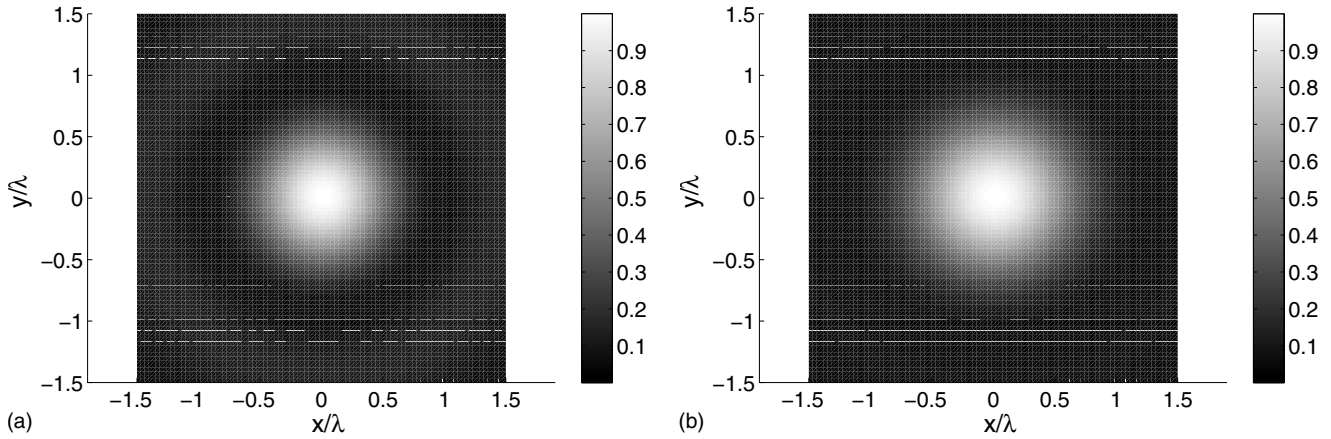

FIG. 1. Left: the normalized distribution of $|E_z|^2$ in the $z=0$ plane for the field with maximum longitudinal component when NA$/n=0.5$ and $P_0=1$ ($\lambda=\lambda_0/n$ is the wavelength in the material with refractive index n). For comparison, the normalized electric energy distribution (78) of the x-polarized focused plane wave is shown at the right for the same numerical aperture. The total flow of power in the z direction is the same for both fields.

$$- E_\varphi(\varrho,\varphi,z)H_\varrho(\varrho,\varphi,z)^*]\hat{\mathbf{z}}\}, \tag{71}$$

with

$$\begin{aligned}\mathrm{Re}\, S_\varrho(\varrho,\varphi,z) &= \frac{1}{2}\,\mathrm{Re}[E_\varphi(\varrho,\varphi,z)H_z(\varrho,\varphi,z)^* \\ &\quad - E_z(\varrho,\varphi,z)H_\varphi(\varrho,\varphi,z)^*] \\ &= \pi^2\frac{n^3}{\Lambda^2\lambda_0^4}\left(\frac{\mu_0}{\epsilon_0}\right)^{1/2}\{2\,\mathrm{Im}[g_1^{1,2}(g_2^{1,1})^*]v_\varrho^2 \\ &\quad - \mathrm{Im}[(g_0^{0,1}+g_0^{2,1}-g_2^{0,3})(g_1^{0,2})^*]v_\varphi^2 \\ &\quad + 2\,\mathrm{Im}[g_0^{0,3}(g_1^{0,2})^*]v_z^2 - 2\,\mathrm{Re}[g_1^{1,2}(g_1^{0,2})^* \\ &\quad - g_0^{0,3}(g_2^{1,1})^*]v_\varrho v_z\},\end{aligned} \tag{72}$$

$$\begin{aligned}\mathrm{Re}\, S_\varphi(\varrho,\varphi,z) &= \frac{1}{2}\,\mathrm{Re}[E_z(\varrho,\varphi,z)H_\varrho(\varrho,\varphi,z)^* \\ &\quad - E_\varrho(\varrho,\varphi,z)H_z(\varrho,\varphi,z)^*] \\ &= \pi^2\frac{n^3}{\Lambda^2\lambda_0^4}\left(\frac{\mu_0}{\epsilon_0}\right)^{1/2}\{\mathrm{Im}[-2g_1^{1,2}(g_2^{1,1})^* + (g_0^{0,1} \\ &\quad + g_0^{2,1}+g_2^{0,3})(g_1^{0,2})^*]v_\varrho v_\varphi - 2\,\mathrm{Re}[g_1^{1,2}(g_1^{0,2})^* \\ &\quad + g_0^{0,3}(g_2^{1,1})^*]v_\varphi v_z\},\end{aligned} \tag{73}$$

$$\begin{aligned}\mathrm{Re}\, S_z(\varrho,\varphi,z) &= \frac{1}{2}\,\mathrm{Re}[E_\varrho(\varrho,\varphi,z)H_\varphi(\varrho,\varphi,z)^* \\ &\quad - E_\varphi(\varrho,\varphi,z)H_\varrho(\varrho,\varphi,z)^*] \\ &= \pi^2\frac{n^3}{\Lambda^2\lambda_0^4}\left(\frac{\mu_0}{\epsilon_0}\right)^{1/2}\{-\mathrm{Re}[(g_0^{0,1}+g_0^{2,1} \\ &\quad + g_1^{0,3})(g_2^{1,1})^*]v_\varrho^2 \\ &\quad + \mathrm{Re}[(g_0^{0,1}+g_0^{2,1}-g_2^{0,3})(g_2^{1,1})^*]v_\varphi^2 \\ &\quad + 2\,\mathrm{Re}[g_1^{1,2}(g_1^{0,2})^*]v_z^2 \\ &\quad - \mathrm{Im}[(g_0^{0,1}+g_0^{2,1}+g_2^{0,3})(g_1^{0,2})^* \\ &\quad + g_1^{1,2}(g_2^{1,1})^*]v_\varrho v_z\}.\end{aligned} \tag{74}$$

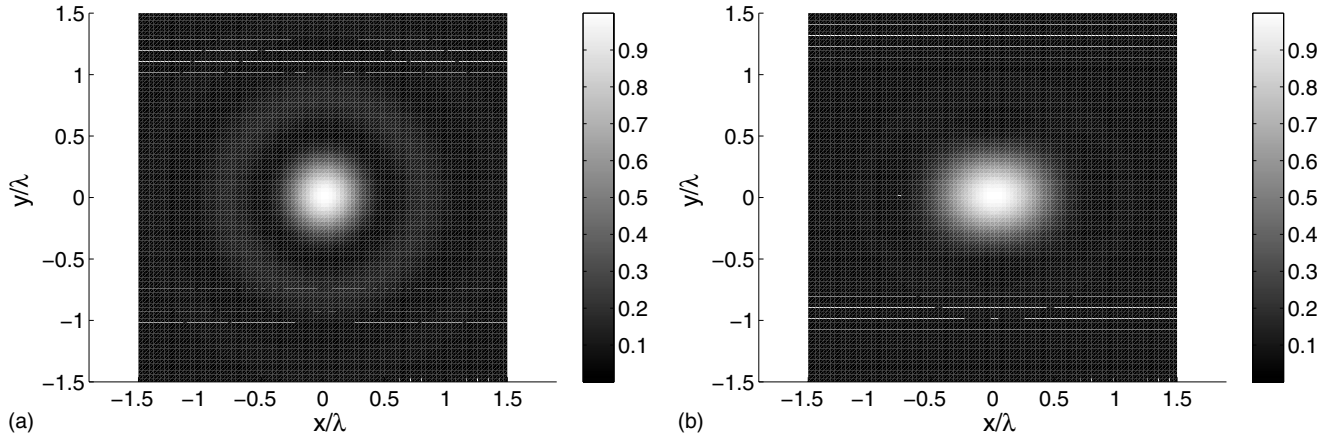

FIG. 2. Same as Fig. 1 except that now NA$/n=0.9$.

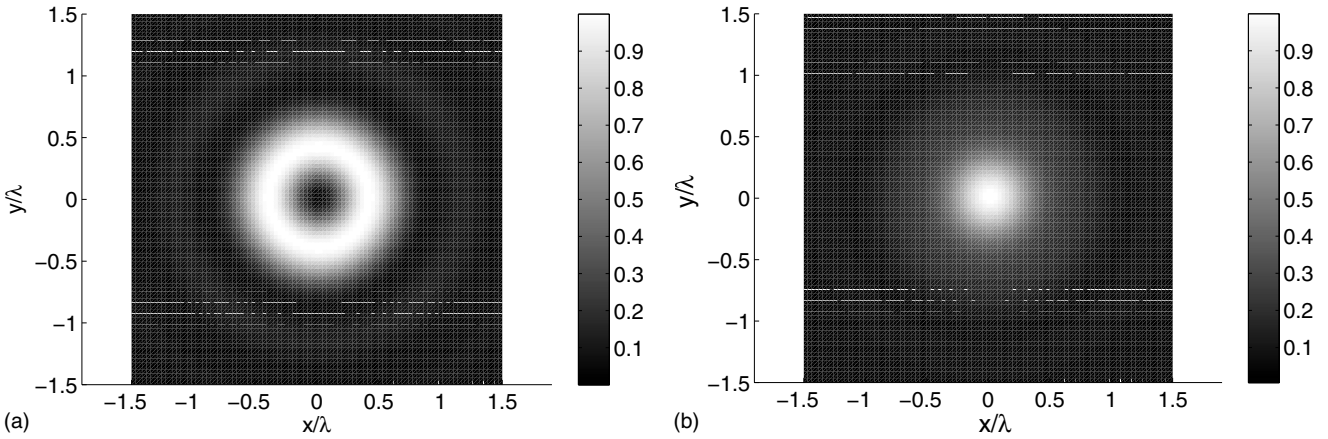

FIG. 3. The squared modulus $|E_\varrho|^2$ of the radial component and electric energy density $|\mathbf{E}|^2$ of the electric field with maximum longitudinal component for NA/n=0.9. The maximum values of $|E_\varrho|^2$ are approximately 25% of the maximum of the squared modulus $|E_z|^2$ of the longitudinal component.

V. OPTIMUM FIELD DISTRIBUTIONS

We will consider now in more detail subsequently fields obtained by optimizing the longitudinal, the transverse, and an intermediate component.

A. Optimum longitudinal component

In this case

$$\hat{\mathbf{v}} = \hat{\mathbf{z}}. \tag{75}$$

Then Eqs. (68) and (70) become

$$\mathbf{E}(\varrho,\varphi,z) = \frac{2\pi n}{\Lambda\lambda_0^2}\left(\frac{\mu_0}{\epsilon_0}\right)^{1/2}[-ig_1^{1,2}(\varrho,z)\hat{\boldsymbol{\varrho}} + g_0^{0,3}(\varrho,z)\hat{\mathbf{z}}], \tag{76}$$

and

$$\mathbf{H}(\varrho,\varphi,z) = -\frac{2\pi i n^2}{\Lambda\lambda_0^2} g_1^{0,2}(\varrho,z)\hat{\boldsymbol{\varphi}}. \tag{77}$$

Since $g_1^{1,2}(0,0)=0$, the electric field in the origin is parallel to the z axis, hence it is purely longitudinal in the origin. In the $z=0$ plane the functions $g_\ell^{\nu,\mu}$ are real and therefore Eq. (76) implies that the polarization ellipse of the electric field in that plane has minor and major axis parallel to the $\hat{\boldsymbol{\varrho}}$ and $\hat{\mathbf{z}}$ axis [which is the major and which the minor axis depends on the relative values of $g_0^{0,3}(\varrho,0)$ and $g_1^{1,2}(\varrho,0)$]. In the $z=0$ plane, the phase of E_z is $\pm\pi$ whereas the other electric field components have phase $\pm\pi/2$. The magnetic field is everywhere parallel to $\hat{\boldsymbol{\varphi}}$, i.e., it is azimuthal. In Fig. 1 the normalized distribution $|E_z(x,y,0)|^2$ of the optimum field with maximum longitudinal component for NA/n=0.5 in the $z=0$ plane is compared to the normalized total electric energy density,

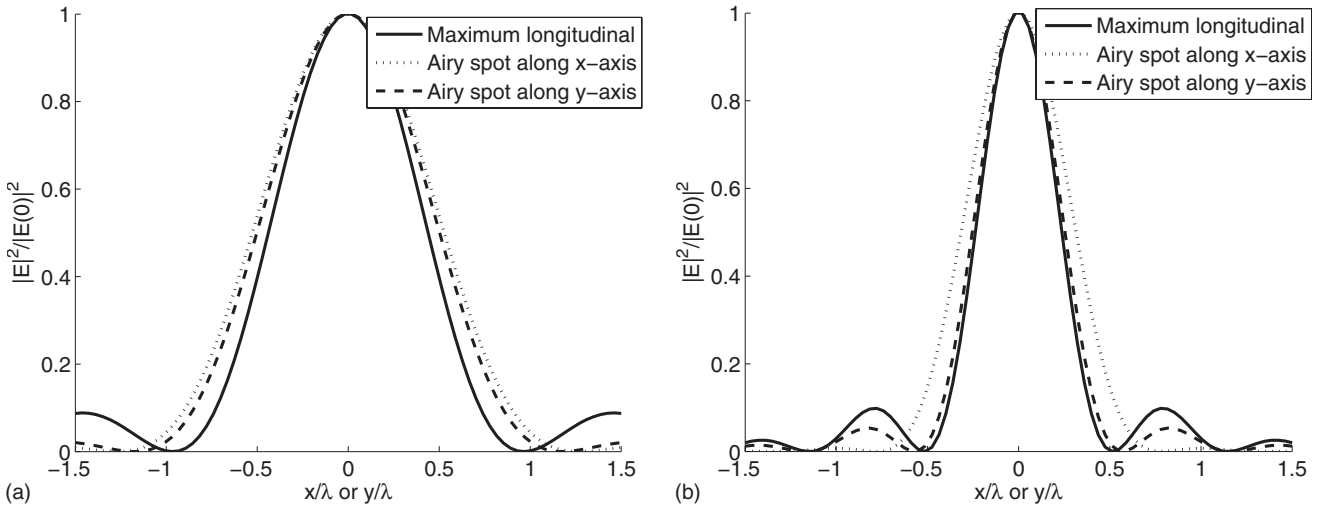

FIG. 4. Cross section of the rotational symmetric $|E_z|^2$ (solid curves) of the field with maximum longitudinal component and cross sections of $|\mathbf{E}(x,0,0)|^2$ (dashed) and $|\mathbf{E}(0,y,0)|^2$ (dotted) of the Airy spot for the x-polarized focused plane wave, for NA/n=0.5 (left) and NA/n=0.9 (right). $\lambda=\lambda_0/n$ and the maxima of all quantities are rescaled to unity.

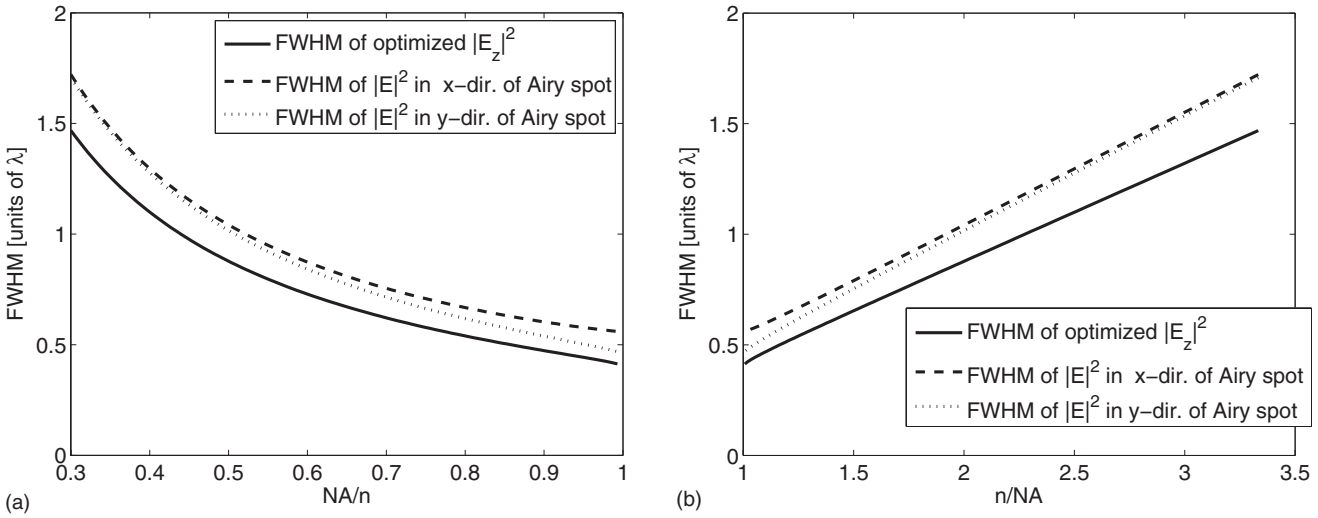

FIG. 5. FWHM of $|E_z(x,y,0)|^2$ of the field with maximum longitudinal component and FWHM of $|\mathbf{E}(x,y,0)|^2$ along the x and y directions of the focused x-polarized plane wave. At the left the FWHM is shown as function of NA/n, at the right as function of n/NA in units of $\lambda=\lambda_0/n$.

$$|E_x(x,y,0)|^2+|E_y(x,y,0)|^2+|E_z(x,y,0)|^2, \tag{78}$$

in the focal plane of the focused x-polarized plane wave. The coordinates x, y are expressed in units of the wavelength $\lambda=\lambda_0/n$ in the material with refractive index n. The formulas for the electric field of a focused plane wave are given in the Appendix [see Eqs. (A14)–(A16)]. The power flow in the z direction of the optimum longitudinal field and the focused plane wave are the same. The distribution of the optimum $|E_z|^2$ is rotationally symmetric while that of the electric energy density, Eq. (78), of the focused linearly polarized plane wave is elliptical, with the short axis parallel to the y direction (i.e., perpendicular to the direction of polarization of the focused plane wave). In Fig. 2 the distributions are compared for NA/n=0.9. In this case the short axis of the elliptic distribution is considerably shorter than the long axis. In Fig. 3 the squared modulus $|E_\varrho|^2$ and $|\mathbf{E}|^2$ are shown. Due to the broad doughnut shaped distribution of the radial component, $|\mathbf{E}|^2$ is broader than the Airy spot.

Cross sections along the short and long axes are shown in Fig. 4 for both NA/n=0.5 and NA/n=0.9. To compare the shapes the maxima of all cross sections are rescaled to 1. It is seen that the longitudinal component has smaller full width at half maximum (FWHM), but also higher secondary maxima.

The FWHM of the optimum longitudinal component is for NA/n=1 almost identical to that of the longitudinal component in [18], obtained by focusing a radially polarized beam using a ring mask function (with radius 90% of the total pupil). However, the side lobes are higher at the cost of the central maximum compared to our longitudinal component. This is of course not surprising because the longitudinal component in [18] was not optimized for a high maximum on the optical axis.

In Fig. 5 the FWHM of $|E_z(x,y,0)|^2$ of the optimum field is compared to the FWHM in the x and y directions of the electric energy density $|\mathbf{E}(x,y,z=0)|^2$ of the focal spot of the x-polarized plane wave. At the left, the FWHM is shown as a function of the numerical aperture NA/n, at the right as a function of n/NA, both in units of wavelength. It is seen that the FWHM of the longitudinal component is smaller than the FWHM in both the x and y directions of the focused spot. The FWHM as a function of n/NA is almost linear, but the slope is smaller for the longitudinal component. This means that the spot size of the optimum longitudinal $|E_z|^2$ is relatively smaller than the Airy spot when the numerical aperture is larger. Nevertheless, for all values of the numerical aperture, the longitudinal spot is narrower than the Airy spot. As shown in Fig. 6, the maximum amplitude $|E_z(\mathbf{0})|$ of the optimum longitudinal component is for most values of the numerical aperture smaller than the maximum amplitude $|E_x(\mathbf{0})|$ of the focused x-polarized plane wave. But for NA/n>0.65 this ratio is already more than 0.5 and for NA/n>0.994 the maximum longitudinal component is even

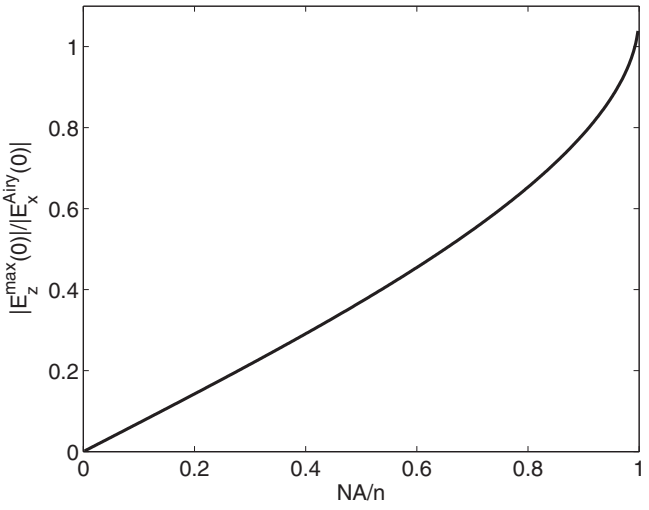

FIG. 6. Ratio of maximum longitudinal amplitude $|E_z|$ and the amplitude $|E_x|$ of the focused x-polarized plane wave for the same power and as a function of NA/n.

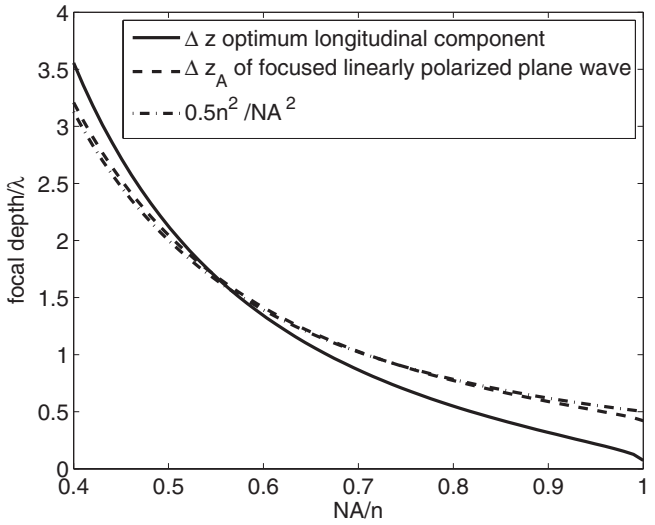

FIG. 7. Focal depth in unit of $\lambda=\lambda_0/n$ as function of NA/n for the optimum longitudinal component and for the energy density of the focused linear polarized plane wave. The approximative scalar paraxial focal depth is also shown in units of λ.

larger than the maximum amplitude $|E_x(\mathbf{0})|$ of the focused x-polarized plane wave.

Along the optical axis we have $\varrho=0$ and

$$g_0^{0,3}(0,z)=\int_0^{\alpha_{\max}} e^{ik_0nz\cos\alpha}\sin^3\alpha d\alpha$$
$$=\frac{i}{k_0nz}\left(1+\frac{2}{k_0^2n^2z^2}\right)[e^{ik_0nz\cos\alpha_{\max}}-e^{ik_0nz}]$$
$$+2\frac{\cos\alpha_{\max}e^{ik_0nz\cos\alpha_{\max}}-e^{ik_0nz}}{k_0^2n^2z^2}$$
$$-i\frac{\cos^2\alpha_{\max}e^{ik_0nz\cos\alpha_{\max}}-e^{ik_0nz}}{k_0nz}. \quad (79)$$

Because $J_1(0)=0$,

$$g_1^{1,2}(0,z)=g_1^{1,2}(0,z)=0. \quad (80)$$

It thus follows from Eq. (76) that along the optical axis the electric field is parallel to the z axis and that the modulus of the field is symmetric with respect to the focal plane. Furthermore,

$$\frac{|E_z(x=0,y=0,z)|^2}{|E_z(0,0,0)|^2}=\frac{|g_0^{0,3}(0,z)|^2}{|g_0^{0,3}(0,0)|^2}, \quad (81)$$

where

$$g_0^{0,3}(0,0)=\frac{2}{3}-\cos\alpha_{\max}+\frac{1}{3}\cos^3\alpha_{\max}. \quad (82)$$

We define the focal depth of the optimum longitudinal component as the distance Δz to the focal plane for which the ratio

$$\frac{|g_0^{0,3}(0,\Delta z)|^2}{|g_0^{0,3}(0,0)|^2}=0.8. \quad (83)$$

For the focused linearly polarized plane wave, the electric energy density on the optical axis is given by Eq. (A40),

$$|\mathbf{E}(x=0,y=0,z)|^2=|E_x(x=0,y=0,z)|^2+|E_y(x=0,y=0,z)|^2$$
$$+|E_z(x=0,y=0,z)|^2$$
$$=\frac{\pi^2n^2f^2}{\lambda_0^2}|g_0^{1/2,1}(0,z)+g_0^{3/2,1}(0,z)|^2. \quad (84)$$

In the origin we have (A41)

$$|\mathbf{E}(0,0,0)|^2=\frac{\pi^2n^2f^2}{\lambda_0^2}\left[\frac{2}{3}(1-\cos^{3/2}\alpha_{\max})\right.$$
$$\left.+\frac{2}{5}(1-\cos^{5/2}\alpha_{\max})\right]^2. \quad (85)$$

The energy density on the optical axis is again symmetric around the focal plane and the focal depth is the distance Δz_A such that

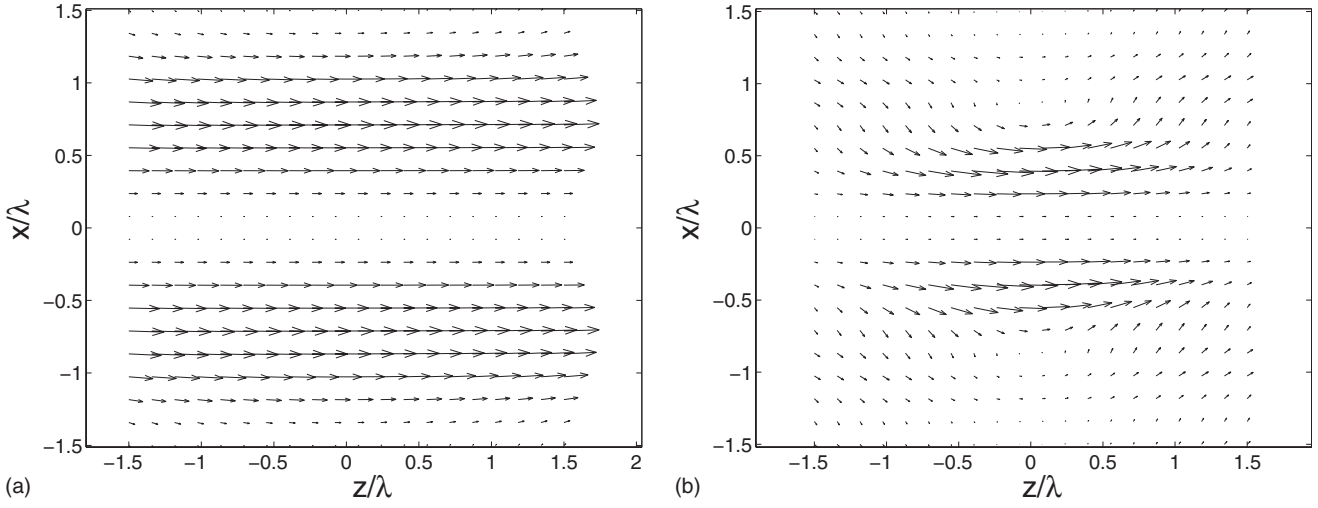

FIG. 8. Poynting vector $\mathbf{S}=S_\varrho\hat{\boldsymbol{\varrho}}+S_z\hat{\mathbf{z}}$ for the fields with maximum longitudinal component, in the (z,x) plane (i.e., the $\varphi=\pi/2$ plane) for $\mathrm{NA}/n=0.5$ (left) and for $\mathrm{NA}/n=0.9$ (right). The Poynting vector is independent of the angular coordinate φ.

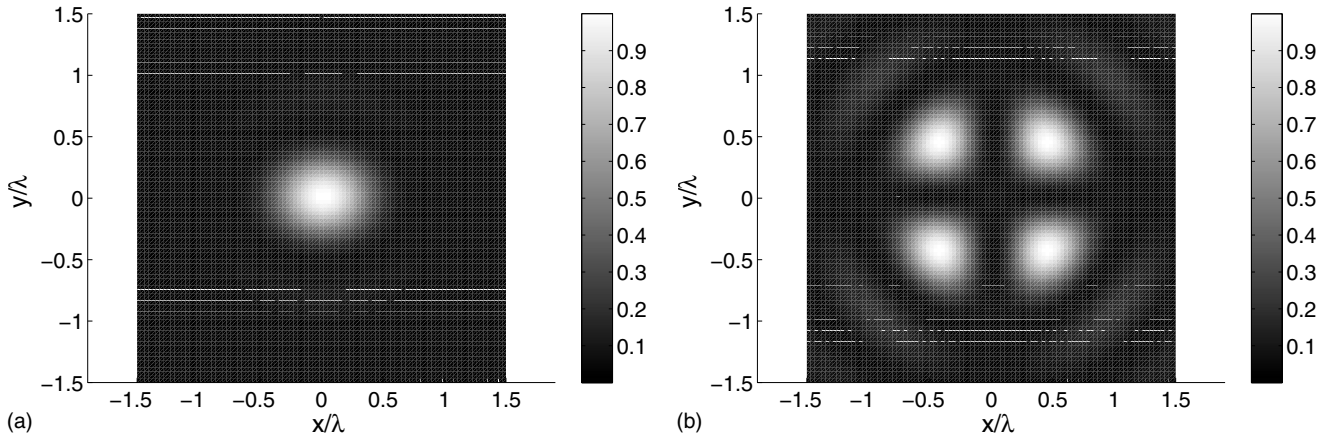

FIG. 9. The normalized distribution of $|E_x|^2$ (left) and $|E_y|^2$ (right) in the $z=0$ plane for the field with optimized x component when $\mathrm{NA}/n=0.9$.

$$\frac{|\mathbf{E}(x=0,y=0,\Delta z_A)|^2}{|\mathbf{E}(0,0,0)|^2}=0.8. \tag{86}$$

Both Δz and Δz_A are shown as functions of NA/n in Fig. 7. The approximative focal depth $0.5\lambda_0 n/\mathrm{NA}^2$, which is valid in the scalar paraxial theory, is also shown. It is seen that for $\mathrm{NA}/n<0.4$ the focal depths of the focused linearly polarized plane wave calculated in the vectorial and the scalar paraxial theory are almost identical. The focal depth of the optimized longitudinal spot is for $\mathrm{NA}/n<0.8$ larger than that of the Airy spot, while for $\mathrm{NA}/n>0.8$ it is smaller.

Equations (72)–(74) imply

$$\mathbf{S}(\varrho,\varphi,z)=\frac{2\pi^2 n^3}{\Lambda^2\lambda_0^4}\left(\frac{\mu_0}{\epsilon_0}\right)^{1/2}(\mathrm{Im}\{g_0^{0,3}(\varrho,z)[g_1^{0,2}(\varrho,z)]^*\}\hat{\boldsymbol{\varrho}}+\mathrm{Re}\{g_1^{1,2}(\varrho,z)[g_1^{0,2}(\varrho,z)]^*\}\hat{\mathbf{z}}). \tag{87}$$

The φ component of the Poynting vector thus vanishes and the Poynting vector is independent of the angle φ. In the $(z=0)$ plane the energy flows in the z direction. In Fig. 8 the time-averaged Poynting vector of the field with maximum longitudinal component is shown in the (z,ϱ) plane for the cases $\mathrm{NA}/n=0.5$ and $\mathrm{NA}/n=0.9$. The φ component of the Poynting vector vanishes and the other components S_ϱ and S_z are independent of rotation angle φ. The Poynting vector vanishes on the z axis.

B. Optimum transverse component

We choose the transverse component parallel to the x axis,

$$\hat{\mathbf{v}}=\hat{\mathbf{x}}, \tag{88}$$

i.e., the x component of the electric field in the origin is optimized. On the local basis (attached to the point of observation) of cylindrical coordinates ϱ, φ, z we have $v_\varrho=\cos\varphi$, $v_\varphi=-\sin\varphi$, $v_z=0$. Hence Eqs. (65), (68), (66), and (70) imply that the optimum electromagnetic field becomes

$$\mathbf{E}(\varrho,\varphi,z)=\frac{\pi n}{\Lambda\lambda_0^2}\left(\frac{\mu_0}{\epsilon_0}\right)^{1/2}\{[g_0^{0,1}(\varrho,z)+g_0^{2,1}(\varrho,z)+g_2^{0,3}(\varrho,z)\cos(2\varphi)]\hat{\mathbf{x}}+g_2^{0,3}(\varrho,z)\sin(2\varphi)\hat{\mathbf{y}}-2ig_1^{0,2}(\varrho,z)\cos\varphi\hat{\mathbf{z}}\} \tag{89}$$

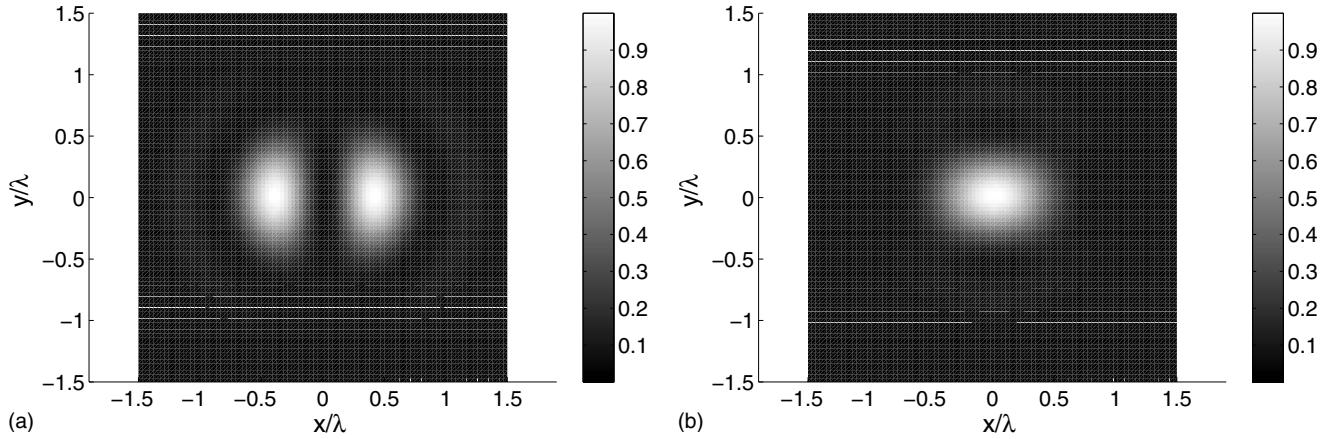

FIG. 10. Normalized distribution of $|E_z|^2$ and of the electric energy density $|\mathbf{E}|^2$ for the field with maximum E_x component $\mathrm{NA}/n=0.9$.

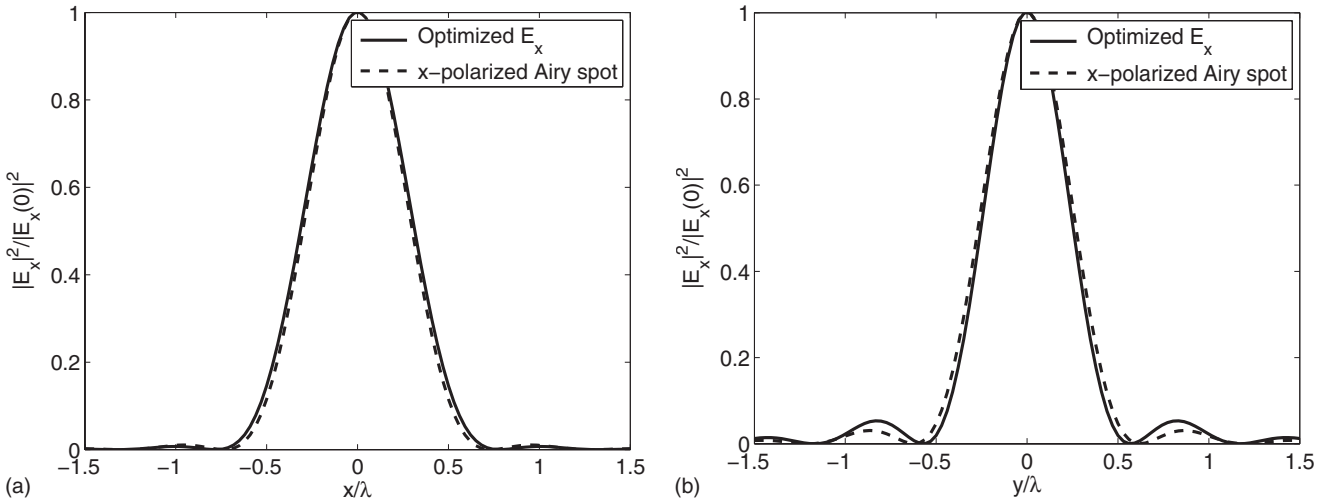

FIG. 11. Cross sections of $|E_x|^2$ along the x (left) and y axis (right) for the field with maximum x component and for the focused x-polarized plane wave with the same power. The numerical aperture is NA/n=0.9. The maxima of all cross sections are rescaled to 1.

$$= \frac{\pi n}{\Lambda \lambda_0^2}\left(\frac{\mu_0}{\epsilon_0}\right)^{1/2}\{[g_0^{0,1}(\varrho,z) + g_0^{2,1}(\varrho,z) + g_2^{0,3}(\varrho,z)]\cos\varphi\hat{\boldsymbol{\varrho}} - [g_0^{0,1}(\varrho,z) + g_0^{2,1}(\varrho,z) - g_2^{0,3}(\varrho,z)]\sin\varphi\hat{\boldsymbol{\varphi}} - 2ig_1^{1,2}(\varrho,z)\cos\varphi\hat{\mathbf{z}}\}, \quad (90)$$

$$\mathbf{H}(\varrho,\varphi,z) = -\frac{2\pi n^2}{\Lambda\lambda_0^2}[g_2^{1,1}(\varrho,z)\sin 2\varphi\hat{\mathbf{x}} - g_2^{1,1}(\varrho,z)\cos 2\varphi\hat{\mathbf{y}} - ig_1^{0,2}(\varrho,z)\sin\varphi\hat{\mathbf{z}}] \quad (91)$$

$$= \frac{2\pi n^2}{\Lambda\lambda_0^2}[g_2^{1,1}(\varrho,z)\sin\varphi\hat{\boldsymbol{\varrho}} - g_2^{1,1}(\varrho,z)\cos\varphi\hat{\boldsymbol{\varphi}} + ig_1^{0,2}(\varrho,z)\sin\varphi\hat{\mathbf{z}}]. \quad (92)$$

The squared amplitudes of the electric field components and the electric energy density in the $z=0$ plane are shown in Figs. 9 and 10 when NA/n=0.9. These field components are very similar to the components of the focused x polarized plane wave for the same NA/n. In Fig. 11 cross sections along the x and y axes of $|E_x|^2$ for the maximum transverse field are the focused linearly polarized plane wave pattern are compared for NA/n=0.9. The maxima of all functions are normalized to 1. Along the y axis, the E_x spot of the optimized transverse field is slightly narrower than for the Airy spot, but has also higher secondary maxima. It can be shown that, just as for the focused x polarized plane wave, E_x of the optimized field is widest along the x axis. In Fig. 12 the FWHM as function of NA/n of $|E_x|^2$ of the optimized field is compared to the FWHM of $|E_x|^2$ of the x-polarized plane wave. The field distributions have elliptical shape. The FWHM is therefore defined with respect to the radial distribution obtained by averaging $|E_x(\varrho,\varphi,z=0)|^2$ over the angle $0<\varphi<2\pi$, as explained in Eq. (A26) in the Appendix. Note that, in contrast to Fig. 5, where the optimum E_z component was compared with the *intensity* of the Airy spot, we here compare the squared moduli of the x components of the electric fields. It is seen that the FWHM of the optimized and the focused plane wave are almost identical.

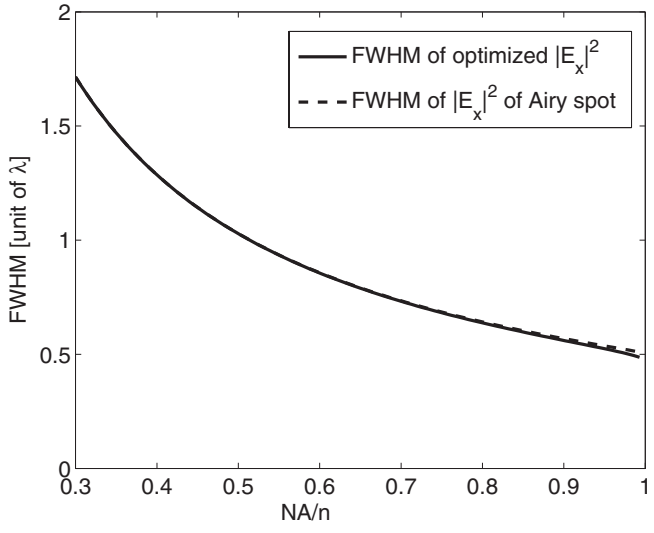

FIG. 12. The FWHM of $|E_x|^2$ along the x axis of the optimized transverse field and the FWHM of the averaged $|E_x|^2$ of the x-polarized focused plane wave.

The optimized electric field at the focal point is pointing in the x direction and is given by

$$E_x(0,0,0) = \sqrt{2\pi P_0}\frac{\sqrt{n}}{\lambda_0}\left(\frac{\mu_0}{\epsilon_0}\right)^{1/4}\left(\frac{4}{3} - \cos\alpha_{\max} - \frac{1}{3}\cos^3\alpha_{\max}\right)^{1/2}. \quad (93)$$

Formulas for the field distributions of the focused x polarized plane wave are derived in the Appendix. For a power given by Eq. (A30), the x component of the electric field in focus is given by Eq. (A41). Hence if the power is P_0 we have for the focused x-polarized plane wave

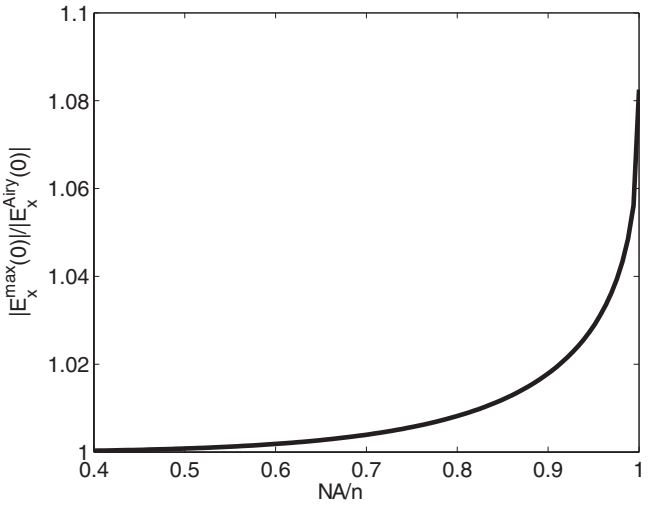

FIG. 13. Ratio of the amplitudes of $E_x(0,0,0)$ at the focal point of the field with maximum $|E_x(0,0,0)|$ and of the focused x-polarized plane wave with the same power. The ratio is for NA $=n$ maximum with value $15/(8\sqrt{3})$.

$$E_x^{plw}(0,0,0) = \sqrt{2\pi P_0}\frac{\sqrt{n}}{\lambda_0}\left(\frac{\mu_0}{\epsilon_0}\right)^{1/4}\frac{1}{\sin\alpha_{\max}} \times\left(\frac{16}{15}-\frac{2}{3}\cos^{3/2}\alpha_{\max}-\frac{2}{5}\cos^{5/2}\alpha_{\max}\right). \tag{94}$$

The ratio of Eqs. (93) and (94),

$$\sin\alpha_{\max}\frac{\left(\frac{4}{3}-\cos\alpha_{\max}-\frac{1}{3}\cos^3\alpha_{\max}\right)^{1/2}}{\frac{16}{15}-\frac{2}{3}\cos^{3/2}\alpha_{\max}-\frac{2}{5}\cos^{5/2}\alpha_{\max}}, \tag{95}$$

is shown in Fig. 13 as function of $\mathrm{NA}/n=\sin\alpha_{\max}$. For $\alpha_{\max}\to 0$ the ratio becomes 1, while for $\alpha_{\max}\to\pi/2$ it becomes $15/(8\sqrt{3})=1.0825$. Hence, the optimized field can have more than 8% higher amplitude E_x than the x-polarized Airy spot of the same power.

C. Intermediate case

Without restricting the generality, we may assume that the vector $\mathbf{v}$ is in the (x,z) plane, i.e., $v_y=0$. It is then convenient to write the optimum focused electric and magnetic field on the orthonormal basis with unit vectors $\hat{\mathbf{v}}$, $\hat{\mathbf{y}}$ and $\hat{\mathbf{v}}\times\hat{\mathbf{y}}$. We have

$$\hat{\mathbf{v}} = v_x\hat{\mathbf{x}}+v_z\hat{\mathbf{z}}, \quad \hat{\mathbf{v}}\times\hat{\mathbf{y}} = -v_z\hat{\mathbf{x}}+v_x\hat{\mathbf{z}}, \tag{96}$$

and therefore

$$\hat{\mathbf{x}} = v_x\hat{\mathbf{v}}-v_z(\hat{\mathbf{v}}\times\hat{\mathbf{y}}), \quad \hat{\mathbf{z}} = v_z\hat{\mathbf{v}}+v_x(\hat{\mathbf{v}}\times\hat{\mathbf{y}}). \tag{97}$$

Hence, Eqs. (65) and (66) become

$$\begin{aligned}\mathbf{E}(\varrho,\varphi,z) &= \pi\frac{n}{\Lambda\lambda_0^2}\left(\frac{\mu_0}{\epsilon_0}\right)^{1/2}(\{[g_0^{0,1}+g_0^{2,1}+g_2^{0,3}\cos(2\varphi)]v_x \\ &\quad -2ig_1^{1,2}\cos\varphi v_z\}\hat{\mathbf{x}}+[g_2^{0,3}\sin(2\varphi)v_x \\ &\quad -2ig_1^{1,2}\sin\varphi v_z]\hat{\mathbf{y}}+[-2ig_1^{1,2}\cos\varphi v_x+2g_0^{0,3}v_z]\hat{\mathbf{z}}) \\ &= \pi\frac{n}{\Lambda\lambda_0^2}\left(\frac{\mu_0}{\epsilon_0}\right)^{1/2}(\{[g_0^{0,1}+g_0^{2,1}+g_2^{0,3}\cos(2\varphi)]v_x^2 \\ &\quad -4ig_1^{1,2}\cos\varphi v_x v_z+2g_0^{0,3}v_z^2\}\hat{\mathbf{v}}+[g_2^{0,3}\sin(2\varphi)v_x \\ &\quad -2ig_1^{1,2}\sin\varphi v_z]\hat{\mathbf{y}}+\{-2ig_1^{1,2}\cos\varphi v_x^2 \\ &\quad -[g_0^{0,1}+g_0^{2,1}-2g_0^{0,3}+g_2^{0,3}\cos(2\varphi)]v_x v_z \\ &\quad +2ig_1^{1,2}\cos\varphi v_z^2\}\hat{\mathbf{v}}\times\hat{\mathbf{y}}),\end{aligned} \tag{98}$$

and

$$\begin{aligned}\mathbf{H}(\varrho,\varphi,z) &= \frac{2\pi n^2}{\Lambda\lambda_0^2}\{[g_2^{1,1}\sin(2\varphi)v_x+ig_1^{0,2}\sin\varphi v_z]\hat{\mathbf{x}} \\ &\quad -[g_2^{1,1}\cos(2\varphi)v_x+ig_1^{0,2}\cos\varphi v_z]\hat{\mathbf{y}} \\ &\quad +ig_1^{0,2}\sin\varphi v_x\hat{\mathbf{z}}\} \\ &= \frac{2\pi n^2}{\Lambda\lambda_0^2}\{[g_2^{1,1}\sin(2\varphi)v_x^2+2ig_1^{0,2}\sin\varphi v_x v_z]\hat{\mathbf{v}}\end{aligned}$$

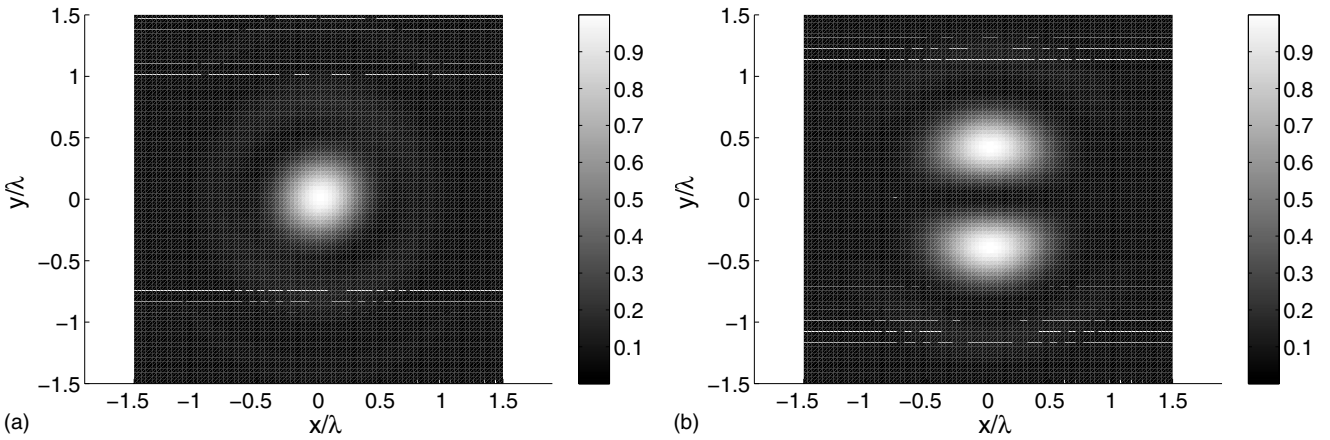

FIG. 14. The normalized distribution of $|E_v|^2$ (left) and $|E_y|^2$ (right) in the $z=0$ plane for the field with optimum field with $\vartheta_v=30°$ when $\mathrm{NA}/n=0.9$.

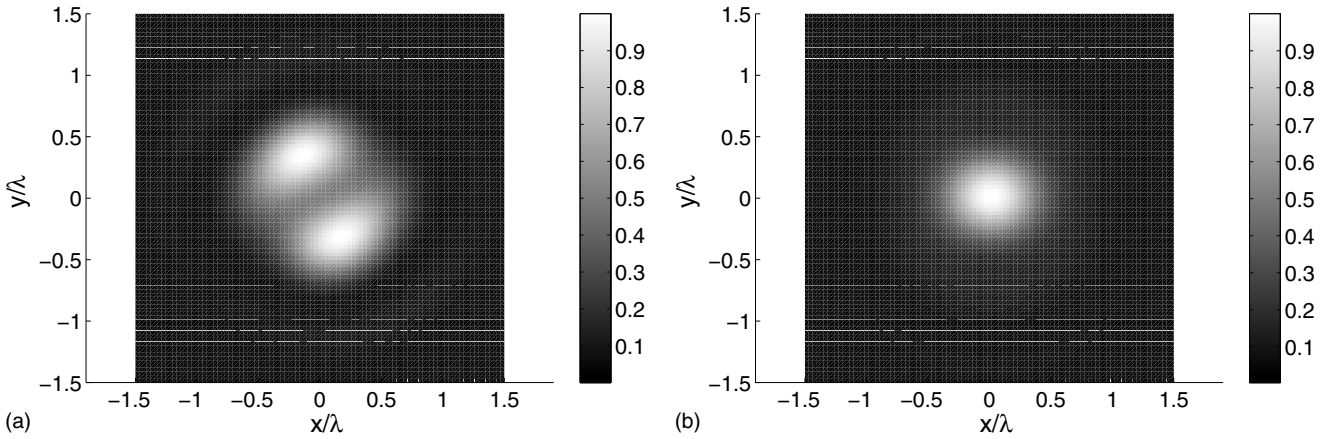

FIG. 15. Normalized distribution of $|E\cdot(\hat{\mathbf{v}}\times\hat{\mathbf{y}})|^2$ and of the electric energy density $|\mathbf{E}|^2$ of the field with maximum v component for $\vartheta_v=30°$ and $\mathrm{NA}/n=0.9$.

$$-[g_2^{1,1}\cos(2\varphi)v_x+ig_1^{0,1}\cos\varphi v_z]\hat{\mathbf{y}}$$
$$+[ig_1^{0,2}\sin\varphi v_x^2-g_2^{1,1}\sin(2\varphi)v_xv_z$$
$$-ig_1^{0,2}\sin\varphi v_z^2]\hat{\mathbf{v}}\times\hat{\mathbf{y}}\}. \quad (99)$$

Because $g_\ell^{\nu,\mu}(0,z)=0$ when $\ell\geqslant 1$, it follows that on the optical axis, $\varrho=0$, we have

$$\mathbf{E}(0,\varphi,z)=\pi\frac{n}{\Lambda\lambda_0^2}\left(\frac{\mu_0}{\epsilon_0}\right)^{1/2}(\{[g_0^{0,1}(0,z)+g_0^{2,1}(0,z)]v_x^2$$
$$+2g_0^{0,3}(0,z)v_z^2\}\hat{\mathbf{v}}-[g_0^{0,1}(0,z)+g_0^{2,1}(0,z)$$
$$-2g_0^{0,3}(0,z)]v_xv_z\hat{\mathbf{v}}\times\hat{\mathbf{y}}), \quad (100)$$

while the magnetic field vanishes there. It follows in particular that the electric field in the origin $\varrho=z=0$ is parallel to $\hat{\mathbf{v}}$ only when $\mathbf{v}$ is perpendicular to the optical axis ($v_z=0$, transverse case) or parallel to it ($v_x=0$ longitudinal case). In all other cases the projection of the electric field at the origin on the plane perpendicular to $\hat{\mathbf{v}}$ is nonzero.

The v component of the electric field is

$$\mathbf{E}(\varrho,\varphi,z)\cdot\hat{\mathbf{v}}=\pi\frac{n}{\Lambda\lambda_0^2}\left(\frac{\mu_0}{\epsilon_0}\right)^{1/2}\{[g_0^{0,1}+g_0^{2,1}+g_2^{0,3}\cos(2\varphi)]v_x^2$$
$$-4ig_1^{1,2}\cos\varphi v_xv_z+2g_0^{0,3}v_z^2\}. \quad (101)$$

In particular, since the functions $g_\ell^{\nu,\mu}$ are all real for $z=0$, we find for the squared modulus of the v component in the $z=0$ plane

$$|\mathbf{E}(\varrho,\varphi,0)\cdot\hat{\mathbf{v}}|^2=\pi^2\frac{n^2}{\Lambda^2\lambda_0^4}\left(\frac{\mu_0}{\epsilon_0}\right)([(g_0^{0,1}+g_0^{2,1}-g_2^{0,3})v_x^2$$
$$+2g_0^{0,3}v_z^2]^2+4\{(g_0^{0,1}+g_0^{2,1}-g_2^{0,3})g_2^{0,3}v_x^4$$
$$+2[g_0^{0,3}g_2^{0,3}+2(g_1^{1,2})^2]v_x^2v_z^2\}\cos^2\varphi$$
$$+4(g_2^{0,3})^2v_x^4\cos^4\varphi), \quad (102)$$

where all $g_l^{\nu,\mu}$ are evaluated at ϱ and $z=0$. If ϑ_v is the angle between the vector $\hat{\mathbf{v}}$ and the positive z axis, we have

$$v_x=\sin\vartheta_v,\quad v_z=\cos\vartheta_v. \quad (103)$$

In Figs. 14 and 15, $|\mathbf{E}\cdot\mathbf{v}|^2$, $|E_y|^2$, $|\mathbf{E}\cdot(\mathbf{v}\times\hat{\mathbf{y}})|^2$ and the electric energy density $|\mathbf{E}|^2$ are shown in the $z=0$ plane for the optimum field with $\vartheta_v=30°$ and $\mathrm{NA}/n=0.9$. Figures 16 and 17

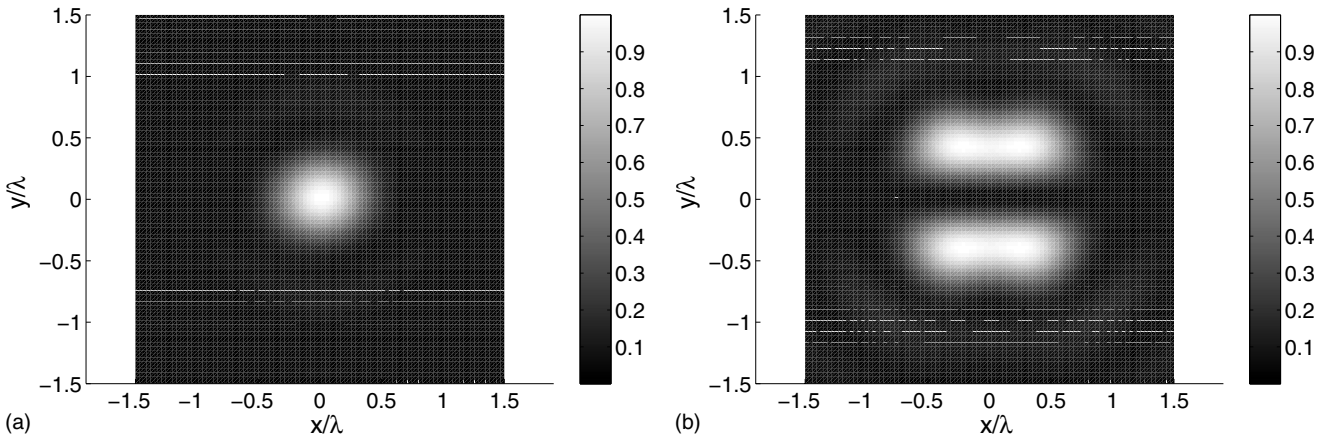

FIG. 16. The normalized distribution of $|E_v|^2$ (left) and $|E_y|^2$ (right) in the $z=0$ plane for the field with optimum field with $\vartheta_v=60°$ when $\mathrm{NA}/n=0.9$.

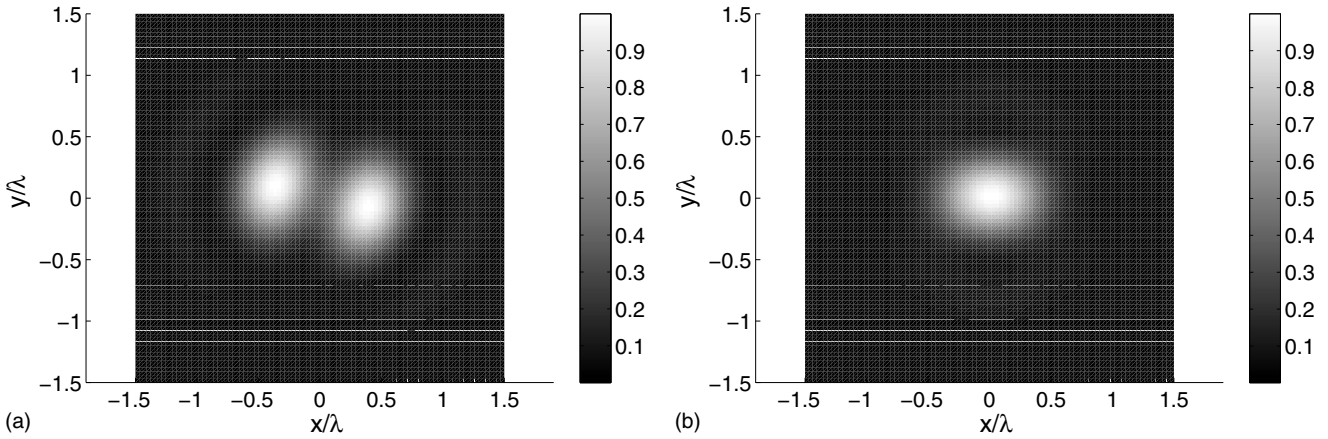

FIG. 17. Normalized distribution of $|E\cdot(\hat{\mathbf{v}}\times\hat{\mathbf{y}})|^2$ and of the electric energy density $|\mathbf{E}|^2$ of the field with maximum v component for $\vartheta_v=60°$ and NA/n=0.9.

correspond to $\vartheta_v=60°$.

In Table I the maxima of the indicated field components in the focal plane are listed for the optimum fields corresponding to NA/n=0.9 for several choices of ϑ_v. In all cases the total flow of power in the pupil of the lens is 1 W.

Equation (102) is a quadratic function of $\cos^2\varphi$ and since the coefficient of $\cos^4\varphi$ is non-negative, it follows that, for every ϱ, the maximum is attained when $\cos^2\varphi=1$, i.e., when $\varphi=0$ and when $\varphi=\pi$. To obtain a useful measure of the spot size, we average Eq. (102) over $0<\varphi<2\pi$,

$$\frac{1}{2\pi}\int_0^{2\pi}|\mathbf{E}(\varrho,\varphi,0)\cdot\hat{\mathbf{v}}|^2d\varphi=\pi^2\frac{n^2}{\Lambda^2\lambda_0^4}\left(\frac{\mu_0}{\epsilon_0}\right)([(g_0^{0,1}+g_0^{2,1}-g_2^{0,3})v_x^2+2g_0^{0,3}v_z^2]^2+2\{(g_0^{0,1}+g_0^{2,1}-g_2^{0,3})g_2^{0,3}v_x^4+2[g_0^{0,3}g_2^{0,3}+2(g_1^{1,2})^2]v_x^2v_z^2\}+\tfrac{3}{2}(g_2^{0,3})^2v_x^4), \tag{104}$$

where we used

$$\frac{1}{2\pi}\int_0^{2\pi}\cos^2\varphi d\varphi=\frac{1}{2},\quad \frac{1}{2\pi}\int_0^{2\pi}\cos^4\varphi d\varphi=\frac{3}{8}. \tag{105}$$

The FWHM in the $z=0$ plane is then defined as the value $2\varrho_0$ such that

TABLE I. Maxima of the optimum electric field components (not of their squares) in the focal plane when NA/n=0.9 and for several choices of the angle ϑ_v. The total power in the lens pupil is in all cases 1 W. Note that the maximum of $|E_y|$ and $|E\cdot(\hat{\mathbf{v}}\times\hat{\mathbf{y}})|$ are not attained at the focal point.

ϑ_v (degrees)	$\lvert E_v\rvert$ (V/m)	$\lvert E_y\rvert$ (V/m)	$\lvert E\cdot(\hat{\mathbf{v}}\times\hat{\mathbf{y}})\rvert$ (V/m)
90°	45.28	6.03	13.67
60°	42.93	7.33	13.81
30°	37.76	14.17	14.04
0°	34.87	17.72	17.72

$$\frac{1}{2\pi}\int_0^{2\pi}|\mathbf{E}(\varrho_0,\varphi,0)\cdot\hat{\mathbf{v}}|^2d\varphi=\frac{1}{2}|\mathbf{E}(0,0,0)\cdot\hat{\mathbf{v}}|^2. \tag{106}$$

In Figs. 18 and 19 the FWHM of $|E_v|$ and the maximum $|E_v(\mathbf{0})|$ are shown as a function of ϑ_v for several values of the numerical aperture and for P_0=1 W. In Fig. 19 the amplitude of $|E_x(\mathbf{0})|$ of the focused x-polarized plane wave is shown for the same power are indicated by the dots. In contrast to the FWHM, the maximum $E_v(\mathbf{0})$ is a monotonically increasing function of ϑ_v.

VI. THE OPTIMUM FIELD IN THE LENS PUPIL

The optimum fields in the $z=0$ plane can be obtained by focusing appropriate pupil distributions. We derive these pupil distributions in this section, using the vector diffraction theory of Ignatowksy and Richards and Wolf. This theory is based on (1) Debye's approximation which expresses the plane wave amplitudes in image space to the field vectors in

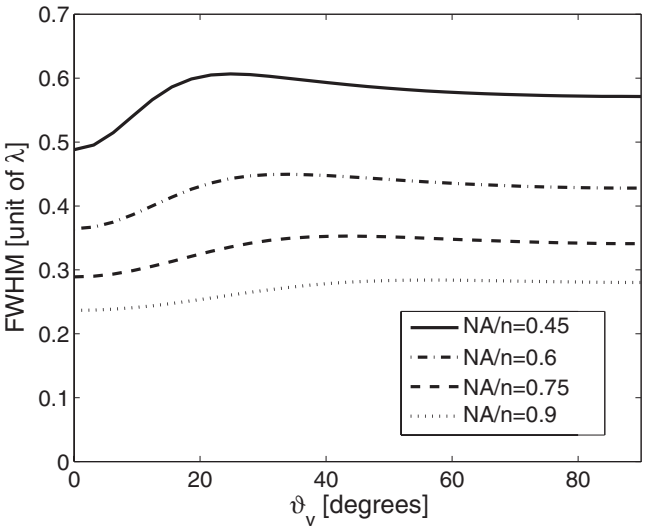

FIG. 18. FWHM expressed in units of $\lambda=\lambda_0/n$ of the optimum $\hat{\mathbf{v}}$ component as function of ϑ_v for several values of NA/n.

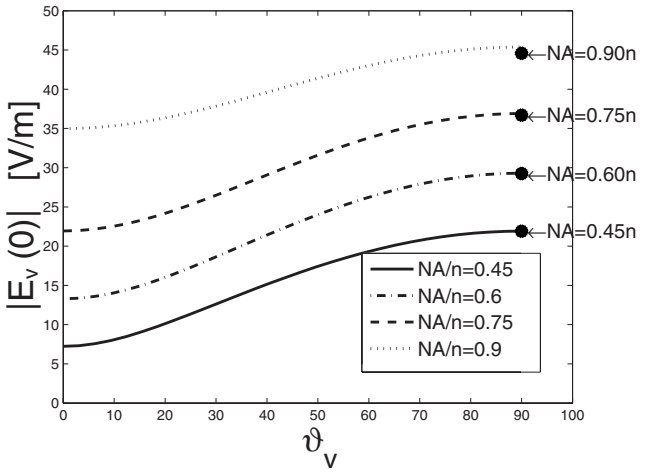

FIG. 19. $|E_v(\mathbf{0})|$ in V/m of the field with optimum $\hat{\mathbf{v}}$ component as function of the angle between $\hat{\mathbf{v}}$ and the z axis (i.e., $\hat{\mathbf{v}}=\sin\vartheta_v\hat{\mathbf{x}}+\cos\vartheta_v\hat{\mathbf{z}}$), for several NA. The power incident on the lens is $P_0=1$ W. The dots are the amplitudes $|E_x(\mathbf{0})|$ of the focused x-polarized plane wave for the same power and the same values of the numerical aperture.

the entrance pupil, and (2) the Abbe's sine condition to guarantee conservation of energy.

Consider a beam that is incident on the pupil of a diffraction limited lens with numerical aperture NA. The electric field in the pupil is given by

$$\mathbf{E}^p(x_p,y_p)=E^p_\varphi(x_p,y_p)\hat{\boldsymbol{\varphi}}_p+E^p_\varrho(x_p,y_p)\hat{\boldsymbol{\varrho}}_p, \tag{107}$$

where x_p and y_p are Cartesian coordinates in the lens pupil, which are parallel to the x and y coordinates of the Cartesian system (x,y,z) in the focal region, and φ_p and ϱ_p are polar coordinates in the pupil,

$$x_p=\varrho_p\cos\varphi_p, \tag{108}$$

$$y_p=\varrho_p\sin\varphi_p, \tag{109}$$

with unit vectors

$$\hat{\boldsymbol{\varrho}}_p=\cos\varphi_p\hat{\mathbf{x}}+\sin\varphi_p\hat{\mathbf{y}}, \tag{110}$$

$$\hat{\boldsymbol{\varphi}}_p=-\sin\varphi_p\hat{\mathbf{x}}+\cos\varphi_p\hat{\mathbf{y}}. \tag{111}$$

According to the theory of Ignatowsky [1,2] and Richards and Wolf [3,4] the field in the pupil of the lens and the amplitude of the plane waves in the focal plane are related by [24]

$$\mathbf{A}(k_x,k_y)=-2\pi i\frac{f}{(k_0n)^{1/2}k_z^{1/2}}\underline{\underline{\mathcal{R}}}(\mathbf{k})\mathbf{E}^p\left(-\frac{fk_x}{k_0n},-\frac{fk_y}{k_0n}\right), \tag{112}$$

where f is the focal distance of the lens and $\underline{\underline{\mathcal{R}}}(\mathbf{k})$ is a matrix which rotates the electric field in the pupil plane in the direction perpendicular to the wave vector $\mathbf{k}=k_0n(\sin\alpha\cos\beta\hat{\mathbf{k}}+\sin\alpha\sin\beta\hat{\boldsymbol{\alpha}}+\cos\alpha\hat{\boldsymbol{\beta}})$,

$$\underline{\underline{\mathcal{R}}}(\mathbf{k})\mathbf{E}^p(x_p,y_p)=-E^p_\varrho(x_p,y_p)\hat{\boldsymbol{\alpha}}-E^p_\varphi(x_p,y_p)\hat{\boldsymbol{\beta}}, \tag{113}$$

with

$$x_p=\varrho_p\cos\varphi_p=-f\frac{k_x}{k_0n}, \tag{114}$$

$$y_p=\varrho_p\sin\varphi_p=-f\frac{k_y}{k_0n}, \tag{115}$$

and $\hat{\boldsymbol{\alpha}}$ and $\hat{\boldsymbol{\beta}}$ are given by Eqs. (8) and (9). Since α and β are the polar and azimuthal angles of the wave vector $\mathbf{k}$,

$$\varrho_p=f\sin\alpha, \tag{116}$$

$$\varphi_p=\beta+\pi. \tag{117}$$

Hence, expressed in terms of α and β,

$$\begin{aligned}\mathbf{A}(\alpha,\beta)&=-2\pi i\frac{f}{k_0n\sqrt{\cos\alpha}}\underline{\underline{\mathcal{R}}}(\alpha,\beta)\mathbf{E}^p(-f\sin\alpha\cos\beta,\\&\quad -f\sin\alpha\sin\beta)\\&=-2\pi i\frac{f}{k_0n\sqrt{\cos\alpha}}[E^p_\varrho(-f\sin\alpha\cos\beta,\\&\quad -f\sin\alpha\sin\beta)\hat{\boldsymbol{\alpha}}+E^p_\varphi(-f\sin\alpha\cos\beta,\\&\quad -f\sin\alpha\sin\beta)\hat{\boldsymbol{\beta}}].\end{aligned} \tag{118}$$

Conversely, given the plane waves amplitudes $\mathbf{A}(k_x,k_y)=A_\alpha\hat{\boldsymbol{\alpha}}+A_\beta\hat{\boldsymbol{\beta}}$ of the field in the focal plane $z=0$, the corresponding field in the pupil of the lens is

$$\mathbf{E}^p(x_p,y_p)=\frac{i}{2\pi}\frac{(k_0n)^{1/2}k_z^{1/2}}{f}\underline{\underline{\mathcal{R}}}(\mathbf{k})^{-1}\mathbf{A}(k_x,k_y), \tag{119}$$

with

$$k_x=-k_0n\frac{x_p}{f},\quad k_y=-k_0n\frac{y_p}{f}, \tag{120}$$

$(x_p^2+y_p^2)^{1/2}\leqslant f\mathrm{NA}/n$ and

$$\underline{\underline{\mathcal{R}}}(\mathbf{k})^{-1}\mathbf{A}=-A_\alpha\hat{\boldsymbol{\varrho}}_p-A_\beta\hat{\boldsymbol{\varphi}}_p. \tag{121}$$

In terms of α, β we obtain

$$\mathbf{E}^p(\varrho_p,\varphi_p)=\frac{i}{2\pi}\frac{k_0n}{f}\cos^{1/2}\alpha\underline{\underline{\mathcal{R}}}(\alpha,\beta)^{-1}\mathbf{A}(\alpha,\beta), \tag{122}$$

where ϱ_p, φ_p and α, β are related by Eqs. (116) and (117). By substituting the expressions for the optimum plane wave coordinates (45) and (46),

$$A_\alpha=\frac{1}{\Lambda n}\left(\frac{\mu_0}{\epsilon_0}\right)^{1/2}\frac{v_\alpha}{\cos\alpha}, \tag{123}$$

$$A_\beta=\frac{1}{\Lambda n}\left(\frac{\mu_0}{\epsilon_0}\right)^{1/2}\frac{v_\beta}{\cos\alpha}, \tag{124}$$

we find

$$\mathbf{E}^p(\varrho_p,\varphi_p) = -\frac{i}{2\pi}\frac{k_0 n}{f}\sqrt{\cos\alpha}(A_\alpha\hat{\boldsymbol{\varrho}}_p + A_\beta\hat{\boldsymbol{\varphi}}_p)$$
$$= -i\frac{1}{\Lambda\lambda_0 f}\left(\frac{\mu_0}{\epsilon_0}\right)^{1/2}\frac{1}{\sqrt{\cos\alpha}}(v_\alpha\hat{\boldsymbol{\varrho}}_p + v_\beta\hat{\boldsymbol{\varphi}}_p), \tag{125}$$

where

$$\Lambda = \sqrt{\frac{\pi}{2}}\frac{n^{1/2}}{P_0^{1/2}\lambda_0}\left(\frac{\mu_0}{\epsilon_0}\right)^{1/4}\left(\frac{4}{3} - \cos\alpha_{\max} - \frac{1}{3}\cos^3\alpha_{\max} - \sin^2\alpha_{\max}\cos\alpha_{\max}v_z^2\right)^{1/2}. \tag{126}$$

Using Eqs. (21) and (22), and

$$\cos\alpha = \frac{\sqrt{f^2-\varrho_p^2}}{f}, \tag{127}$$

$$\sin\alpha = \frac{\varrho_p}{f}, \tag{128}$$

$$\beta = \phi_p - \pi, \tag{129}$$

we obtain

$$\mathbf{E}^p(\varrho_p,\varphi_p) = -\frac{i}{\Lambda\lambda_0 f}\left(\frac{\mu_0}{\epsilon_0}\right)^{1/2}[(v_x\cos\alpha\cos\beta + v_y\cos\alpha\sin\beta - v_z\sin\alpha)\hat{\boldsymbol{\varrho}}_p + (-v_x\sin\beta + v_y\cos\beta)\hat{\boldsymbol{\varphi}}_p]\frac{1}{\sqrt{\cos\alpha}}$$
$$= \frac{i}{\Lambda\lambda_0 f}\left(\frac{\mu_0}{\epsilon_0}\right)^{1/2}\left\{\left[\frac{\sqrt{f^2-\varrho_p^2}}{f}(v_x\cos\varphi_p + v_y\sin\varphi_p) + \frac{\varrho_p}{f^{1/2}(f^2-\varrho_p^2)^{1/4}}v_z\right]\hat{\boldsymbol{\varrho}}_p + \frac{f^{1/2}}{(f^2-\varrho_p^2)^{1/4}}(-v_x\sin\varphi_p + v_y\cos\varphi_p)\hat{\boldsymbol{\varphi}}_p\right\}$$
$$= \frac{i}{\Lambda\lambda_0 f}\left(\frac{\mu_0}{\epsilon_0}\right)^{1/2}\left[\left(\frac{\sqrt{f^2-\varrho_p^2}}{f}v_\varrho + \frac{\varrho_p}{f^{1/2}(f^2-\varrho_p^2)^{1/4}}v_z\right)\hat{\boldsymbol{\varrho}}_p + \frac{f^{1/2}}{(f^2-\varrho_p^2)^{1/4}}v_\varphi\hat{\boldsymbol{\varphi}}_p\right], \tag{130}$$

where v_ϱ, v_φ are the components of the vector $\mathbf{v}$ on the polar basis $\hat{\boldsymbol{\varrho}}_p$, $\hat{\boldsymbol{\varphi}}_p$ in the pupil. It is seen that the optimum electric field in the pupil is linearly polarized with the direction of polarization and amplitude that depend on the radial coordinate only.

In the case of the maximum longitudinal component, $v_\varrho = v_\varphi = 0$, $v_z = 1$, this becomes

$$\mathbf{E}^p(\varrho_p,\varphi_p) = \frac{i}{\Lambda\lambda_0 f}\left(\frac{\mu_0}{\epsilon_0}\right)^{1/2}\frac{\varrho_p}{f^{1/2}(f^2-\varrho_p^2)^{1/4}}\hat{\boldsymbol{\varrho}}_p, \tag{131}$$

whereas for the maximum x component, $v_\varrho = \cos\varphi_p$, $v_\varphi = -\sin\varphi_p, v_z = 0$,

$$\mathbf{E}^p(\varrho_p,\varphi_p) = \frac{i}{\Lambda\lambda_0 f}\left(\frac{\mu_0}{\epsilon_0}\right)^{1/2}\left[\frac{\sqrt{f^2-\varrho_p^2}}{f}\cos\varphi_p\hat{\boldsymbol{\varrho}}_p - \frac{f^{1/2}}{(f^2-\varrho_p^2)^{1/4}}\sin\varphi_p\hat{\boldsymbol{\varphi}}_p\right]$$
$$= \frac{i}{\Lambda\lambda_0 f}\left(\frac{\mu_0}{\epsilon_0}\right)^{1/2}\left[\left(\frac{\sqrt{f^2-\varrho_p^2}}{f}\cos^2\varphi_p + \frac{f^{1/2}}{(f^2-\varrho_p^2)^{1/4}}\sin^2\varphi_p\right)\hat{\mathbf{x}} + \frac{1}{2}\left(\frac{\sqrt{f^2-\varrho_p^2}}{f} - \frac{f^{1/2}}{(f^2-\varrho_p^2)^{1/4}}\right)\sin 2\varphi_p\hat{\mathbf{y}}\right]. \tag{132}$$

One may have expected that the maximum longitudinal component is obtained by concentrating the radially polarized pupil field in a small annular ring at the rim of the pupil. Instead, the optimum field amplitude (131) increases continuously from zero at the center to a maximum at the rim of the pupil. This is due to the fact that the total power is an integral over the pupil of the squared amplitude of the field while the longitudinal component in the focal point is the integral over the pupil of the field itself. If the radially polarized pupil field is concentrated in a ring of width $\delta\varrho_p = f\mathrm{NA}\,\delta\alpha$, the longitudinal field component in the focal plane becomes approximately

$$E_z(\varrho,\varphi,0) \propto J_0(k_0 n\varrho n\mathrm{NA})(\delta\alpha)^{1/2}. \tag{133}$$

The longitudinal component thus becomes in the limit $\delta\alpha \to 0$ proportional to $J_0(k_0 n\varrho\mathrm{NA})$ and hence decreases slowly as $1/\sqrt{k_0\varrho}$ for increasing distance ϱ to the optical axis. To keep the total power finite, the amplitude vanishes with the square root of the width of the annular ring. The FWHM of the squared amplitude decreases with the width of the ring and has minimum value of $0.35\lambda_0/(n\mathrm{NA})$ for $\delta\alpha \to 0$. But for small widths the side lobes are relatively strong, the first maximum adjacent to the center having squared amplitude that is 16% of the central maximum.

Suppose now that the vector $\hat{\mathbf{v}}$ is in the (x,z) plane and the angle with the positive z axis is ϑ_v. Then Eq. (103) holds and Eq. (130) becomes

$$\mathbf{E}^p(\varrho_p,\varphi_p) = \frac{i}{\sqrt{2}\Lambda\lambda_0 f}\left(\frac{\mu_0}{\epsilon_0}\right)^{1/2}\left[\left(\frac{\sqrt{f^2-\varrho_p^2}}{f}\cos\varphi_p\sin\vartheta_v + \frac{\varrho_p}{f^{1/2}(f^2-\varrho_p^2)^{1/4}}\cos\vartheta_v\right)\hat{\boldsymbol{\varrho}}_p - \frac{f^{1/2}}{(f^2-\varrho_p^2)^{1/4}}\sin\varphi_p\sin\vartheta_v\hat{\boldsymbol{\varphi}}_p\right]. \tag{134}$$

The pupil field is always linearly polarized, with the direction of polarization that varies with the pupil point. The

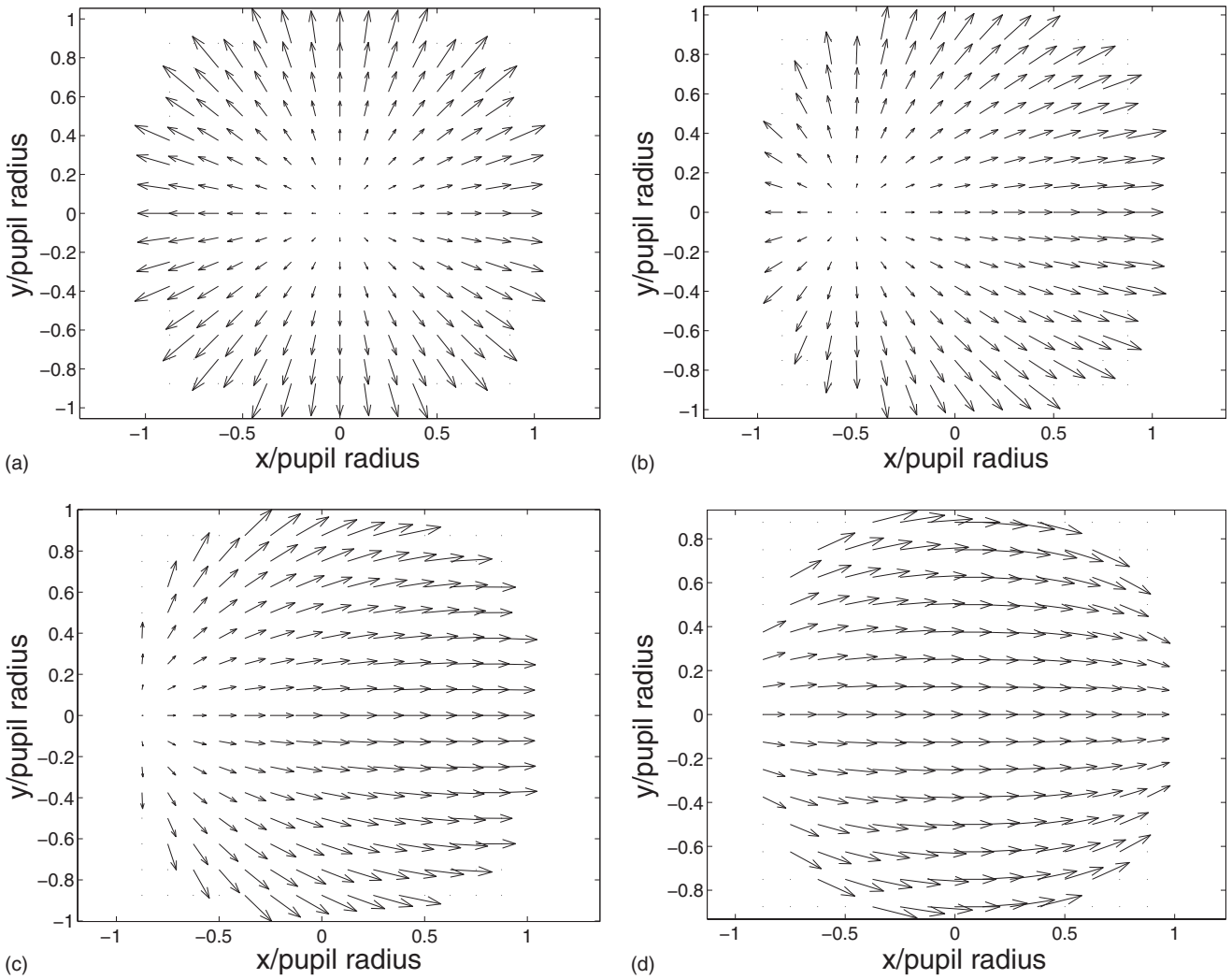

FIG. 20. Snapshot of the electric filed in the pupil that, when focused, yields the field with maximum v component in focus when NA/n=0.9. The upper left figure corresponds to ϑ_v=0°, the upper right to ϑ_v=30°, the lower left to ϑ_v=60°, and the lower right ϑ_v=90°.

phase of the field is the same in all points of the pupil. In Fig. 20 we show snapshots of the electric field in the pupil for ϑ_v=0 (i.e., the longitudinal component in focus is maximum), ϑ_v=90° (i.e., the x component in focus is maximum), and the intermediate cases ϑ_v=30° and ϑ_v=60°. In all cases NA/n=0.9. For ϑ_v=0 the electric field is radially polarized, for ϑ_v=90° it is the field of a plane wave polarized parallel to the x axis. For ϑ_v=30° and ϑ_v=60° intermediate cases occur. In Fig. 21 the squared modulus of the electric pupil field is shown as function of the normalized pupil coordinate $\bar{\varrho}_p=\varrho_p/a$, with $a=f\mathrm{NA}/n$, for several values of NA/n and for ϑ_v=0° (i.e., the pupil fields correspond to fields with maximum longitudinal component). The square modulus shown has been rescaled by the factor a^2, hence the function

$$\bar{\varrho}_p \mapsto a^2|\mathbf{E}(a\bar{\varrho}_p)|^2, \tag{135}$$

is shown. The reason is that the power in the pupil is proportional to the following integral over the normalized radial pupil coordinate,

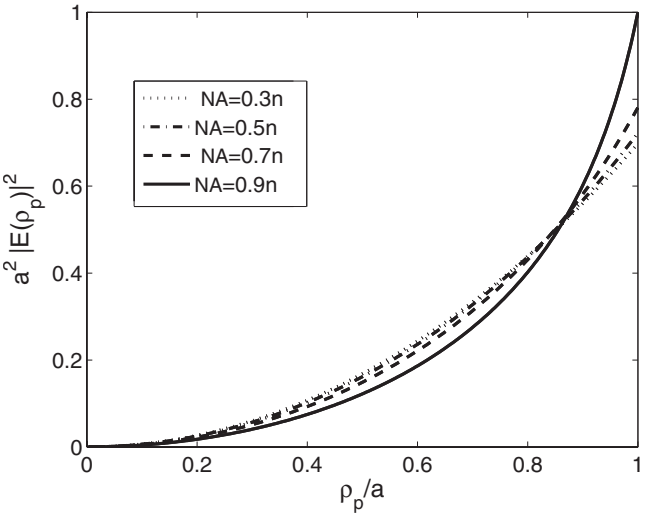

FIG. 21. Electric energy density $a^2|\mathbf{E}(\varrho_p)|^2$ in the lens pupil as function of the radial coordinate ϱ_p, corresponding to the maximum longitudinal component in focus for several NA/n. All values are relative to the value for NA/n=0.9 at the rim of the pupil.

$$\int_0^1 a^2 |\mathbf{E}(a\bar{\varrho}_p)|^2 \bar{\varrho}_p d\bar{\varrho}_p. \tag{136}$$

It is seen that for higher NA/n the electric energy density is more concentrated near the rim of the pupil. But even for NA/n=0.9, the energy density is smoothly varying inside the pupil. Hence it seems quite possible to realize these pupil fields using appropriately programmed spatial light modulators. It may be important in some applications to realize the radially increasing amplitude without absorbing a substantial part of the light. This could be done with optical elements which refract energy close to the axis towards the rim of the pupil.

VII. DISCUSSION

We have studied fields which, with respect to some Cartesian coordinate system (x,y,z), consist of plane waves that all propagate in the positive z direction in a homogeneous isotropic lossless medium with refractive index n. The sinus of the maximum angle between the plane wave vectors and the z axis is the numerical aperture of the plane wave superposition. Let $\hat{\mathbf{v}}$ be a unit vector. For given $\hat{\mathbf{v}}$, given NA and given mean power flow in the positive z direction, we have determined closed formulas for the plane wave amplitudes for which the projection of the electric field in the direction of $\hat{\mathbf{v}}$ in the origin is larger or equal than that of all fields with the same NA and the same maximum power flow. Closed formulas have been derived for the plane wave amplitudes. By choosing $\hat{\mathbf{v}}$ parallel to the z axis, we obtain the field for which the amplitude of the longitudinal component is maximum. The width of this longitudinal component is considerably smaller than that of the Airy spot for the same power and the same NA. By choosing $\mathbf{v}$ perpendicular to the z axis, along the x axis say, we obtain the field for which the amplitude of the x component of the electric field in the origin is maximum. This field is similar to the field of a focused linearly polarized plane, but it is not identical to it. Also for directions of $\hat{\mathbf{v}}$ that are intermediate between longitudinal and transverse, the optimum fields were studied. In particular the FWHM of the components in the plane z=0 where compared for several values of the numerical aperture.

By using the vectorial diffraction theory of Ignatowsky and Richards and Wolf, the field distributions in the pupil of a diffraction-limited lens of given NA was derived such that the focused are the previously discussed fields for which the projection of the electric field along the $\hat{\mathbf{v}}$ direction is maximum in the focal point. Closed formulas were obtained. When $\hat{\mathbf{v}}$ is chosen equal to the unit vector along the z axis, the pupil field is radially polarized. When $\hat{\mathbf{v}}$ is parallel to the x direction, the pupil field is almost identical to that of a plane wave that is polarized parallel to the x direction. In general, the pupil fields that yield the optimum fields near the focal plane are linearly polarized and in phase in all points of the pupil. But the state of polarization and the amplitude varies with position in the pupil.

APPENDIX: THE FOCUSED FIELD OF A LINEARLY POLARIZED PLANE WAVE

We recall here the expression for the electric field near the focal plane of a linearly polarized plane wave in the pupil of a lens of numerical aperture NA, as derived in the theory of Ignatowsky [1,2] and Richards and Wolf [3,4]. With respect to the polar basis, the x-polarized pupil field can be written

$$\mathbf{E}^p(\varrho_p,\varphi_p) = E^p_\varrho(\varrho_p,\varphi_p)\hat{\boldsymbol{\varrho}}_p + E^p_\varphi(\varrho_p,\varphi_p)\hat{\boldsymbol{\varphi}}_p, \tag{A1}$$

with

$$\hat{\boldsymbol{\varrho}}_p = \cos\varphi_p\hat{\mathbf{x}} + \sin\varphi_p\hat{\mathbf{y}}, \tag{A2}$$

$$\hat{\boldsymbol{\varphi}}_p = -\sin\varphi_p\hat{\mathbf{x}} + \cos\varphi_p\hat{\mathbf{y}}, \tag{A3}$$

and

$$E^p_\varrho(\varrho_p,\varphi_p) = \cos\varphi_p, \tag{A4}$$

$$E^p_\varphi(\varrho_p,\varphi_p) = -\sin\varphi_p. \tag{A5}$$

According to Eqs. (18) and (19), the plane wave expansion of the electromagnetic field near the focal plane can be written as

$$\mathbf{E}(\mathbf{r}) = \frac{n^2}{\lambda_0^2}\int_0^{\alpha_{\max}}\int_0^{2\pi}(A_\alpha\hat{\boldsymbol{\alpha}} + A_\beta\hat{\boldsymbol{\beta}})\sin\alpha\cos\alpha e^{i\mathbf{k}\cdot\mathbf{r}}d\alpha d\beta, \tag{A6}$$

$$\mathbf{H}(\mathbf{r}) = \frac{n^3}{\lambda_0^2}\left(\frac{\epsilon_0}{\mu_0}\right)^{1/2}\int_0^{\alpha_{\max}}\int_0^{2\pi}(-A_\beta\hat{\boldsymbol{\alpha}} + A_\alpha\hat{\boldsymbol{\beta}})\sin\alpha\cos\alpha e^{i\mathbf{k}\cdot\mathbf{r}}d\alpha d\beta, \tag{A7}$$

where α and β are spherical coordinates for the wave vectors of the plane waves,

$$\mathbf{k} = k_0 n(\cos\beta\sin\alpha\hat{\mathbf{x}} + \sin\beta\sin\alpha\hat{\mathbf{y}} + \cos\alpha\hat{\mathbf{z}}), \tag{A8}$$

and $\hat{\boldsymbol{\alpha}}$ and $\hat{\boldsymbol{\beta}}$ are given by Eqs. (8) and (9). With respect to cylindrical coordinates $\mathbf{r}=\varrho\hat{\varrho}+z\hat{\mathbf{z}}$, we have

$$\mathbf{k}\cdot\mathbf{r} = k_0 n[\varrho\sin\alpha\cos(\beta-\varphi) + z\cos\alpha]. \tag{A9}$$

By substituting Eqs. (A4) and (A5) into Eq. (118) and using Eq. (117), $\varphi_p=\beta+\pi$, we find

$$A_\alpha(\alpha,\beta) = 2\pi i\frac{f}{k_0 n}\frac{\cos\beta}{\sqrt{\cos\alpha}}, \tag{A10}$$

$$A_\beta(\alpha,\beta) = -2\pi i\frac{f}{k_0 n}\frac{\sin\beta}{\sqrt{\cos\alpha}}. \tag{A11}$$

Hence,

$$\mathbf{A}(\alpha,\beta) = 2\pi i\frac{f}{k_0 n\sqrt{\cos\alpha}}[\cos\beta\hat{\boldsymbol{\alpha}} - \sin\beta\hat{\boldsymbol{\beta}}]$$

$$= 2\pi i\frac{f}{k_0 n\cos^{1/2}\alpha}\{(\cos\alpha\cos^2\beta + \sin^2\beta)\hat{\mathbf{x}} + (\cos\alpha - 1)\cos\beta\sin\beta\hat{\mathbf{y}} - \sin\alpha\cos\beta\hat{\mathbf{z}}\}, \tag{A12}$$

and

$$-A_\beta\hat{\boldsymbol{\alpha}}+A_\alpha\hat{\boldsymbol{\beta}}=2\pi i\frac{f}{k_0n\sqrt{\cos\alpha}}[\sin\beta\hat{\boldsymbol{\alpha}}+\cos\beta\hat{\boldsymbol{\beta}}]$$
$$=2\pi i\frac{f}{k_0n\sqrt{\cos\alpha}}[(\cos\alpha-1)\cos\beta\sin\beta\hat{\mathbf{x}}+(\cos\alpha\sin^2\beta+\cos^2\beta)\hat{\mathbf{y}}-\sin\alpha\cos\beta\hat{\mathbf{z}}], \quad \text{(A13)}$$

where f is the focal length. Substitution into plane wave expansion (A6) and using formulas (59)–(64) yields

$$E_x(\mathbf{r})=\frac{i\pi nf}{\lambda_0}\{g_0^{1/2,1}(\varrho,z)+g_0^{3/2,1}(\varrho,z)+[g_2^{1/2,1}(\varrho,z)-g_2^{3/2,1}(\varrho,z)]\cos 2\varphi\}, \quad \text{(A14)}$$

$$E_y(\mathbf{r})=\frac{i\pi nf}{\lambda_0}[g_2^{1/2,1}(\varrho,z)-g_2^{3/2,1}(\varrho,z)]\sin 2\varphi, \quad \text{(A15)}$$

$$E_z(\mathbf{r})=\frac{2\pi nf}{\lambda_0}g_1^{1/2,2}(\varrho,z)\cos\varphi, \quad \text{(A16)}$$

and

$$H_x(\mathbf{r})=\frac{i\pi n^2f}{\lambda_0}\sqrt{\frac{\epsilon_0}{\mu_0}}[g_2^{1/2,1}(\varrho,z)-g_2^{3/2,1}(\varrho,z)]\sin(2\varphi), \quad \text{(A17)}$$

$$H_y(\mathbf{r})=\frac{i\pi n^2f}{\lambda_0}\sqrt{\frac{\epsilon_0}{\mu_0}}\{g_0^{1/2,1}(\varrho,z)+g_0^{3/2,1}(\varrho,z)-[g_2^{1/2,1}(\varrho,z)-g_2^{3/2,1}(\varrho,z)]\cos(2\varphi)\}, \quad \text{(A18)}$$

$$H_z(\mathbf{r})=\frac{2\pi n^2f}{\lambda_0}\sqrt{\frac{\epsilon_0}{\mu_0}}g_1^{1/2,2}(\varrho,z)\sin\varphi. \quad \text{(A19)}$$

The cylindrical field components are

$$E_\varrho(\mathbf{r})=E_x(\mathbf{r})\cos\varphi+E_y(\mathbf{r})\sin\varphi$$
$$=\frac{i\pi nf}{\lambda_0}[g_0^{1/2,1}(\varrho,z)+g_0^{3/2,1}(\varrho,z)+g_2^{1/2,1}(\varrho,z)-g_2^{3/2,1}(\varrho,z)]\cos\varphi, \quad \text{(A20)}$$

$$E_\varphi(\mathbf{r})=-E_x(\mathbf{r})\sin\varphi+E_y(\mathbf{r})\cos\varphi$$
$$=-\frac{i\pi nf}{\lambda_0}[g_0^{1/2,1}(\varrho,z)+g_0^{3/2,1}(\varrho,z)-g_2^{1/2,1}(\varrho,z)+g_2^{3/2,1}(\varrho,z)]\sin\varphi, \quad \text{(A21)}$$

and

$$H_\varrho(\mathbf{r})=H_x(\mathbf{r})\cos\varphi+H_y(\mathbf{r})\sin\varphi$$
$$=\frac{i\pi n^2f}{\lambda_0}\sqrt{\frac{\epsilon_0}{\mu_0}}[g_0^{1/2,1}(\varrho,z)+g_0^{3/2,1}(\varrho,z)+g_2^{1/2,1}(\varrho,z)-g_2^{3/2,1}(\varrho,z)]\sin\varphi, \quad \text{(A22)}$$

$$H_\varphi(\mathbf{r})=-H_x(\mathbf{r})\sin\varphi+H_y(\mathbf{r})\cos\varphi$$
$$=\frac{i\pi n^2f}{\lambda_0}\sqrt{\frac{\epsilon_0}{\mu_0}}[g_0^{1/2,1}(\varrho,z)+g_0^{3/2,1}(\varrho,z)-g_2^{1/2,1}(\varrho,z)+g_2^{3/2,1}(\varrho,z)]\cos\varphi. \quad \text{(A23)}$$

In the plane $z=0$ all functions $g_\ell^{\nu,\mu}$ are real. Therefore, the squared modulus of the electric field in the $z=0$ plane is

$$|\mathbf{E}(\varrho,\varphi,0)|^2=|E_\varrho(\varrho,\varphi,0)|^2+|E_\varphi(\varrho,\varphi,0)|^2+|E_z(\varrho,\varphi,0)|^2$$
$$=\frac{\pi^2n^2f^2}{\lambda_0^2}\{[g_0^{1/2,1}(\varrho,0)+g_0^{3/2,1}(\varrho,0)+g_2^{1/2,1}(\varrho,0)-g_2^{3/2,1}(\varrho,0)]^2\cos^2\varphi+[g_0^{1/2,1}(\varrho,0)+g_0^{3/2,1}(\varrho,0)-g_2^{1/2,1}(\varrho,0)+g_2^{3/2,1}(\varrho,0)]^2\sin^2\varphi+[g_1^{1/2,2}(\varrho,0)]^2\cos^2\varphi\}. \quad \text{(A24)}$$

The spot shape is elliptical. To obtain a measure of the spot size we average the squared modulus over $0<\varphi<2\pi$,

$$\frac{1}{2\pi}\int_0^{2\pi}|\mathbf{E}(\varrho,\varphi,0)|^2d\varphi=\frac{\pi^2n^2f^2}{2\lambda_0^2}\{[g_0^{1/2,1}(\varrho,0)+g_0^{3/2,1}(\varrho,0)+g_2^{1/2,1}(\varrho,0)-g_2^{3/2,1}(\varrho,0)]^2+[g_0^{1/2,1}(\varrho,0)+g_0^{3/2,1}(\varrho,0)-g_2^{1/2,1}(\varrho,0)+g_2^{3/2,1}(\varrho,0)]^2+[g_1^{1/2,2}(\varrho,0)]^2\}$$
$$=\frac{\pi^2n^2f^2}{\lambda_0^2}\left\{[g_0^{1/2,1}(\varrho,0)+g_0^{3/2,1}(\varrho,0)]^2+[g_2^{1/2,1}(\varrho,0)-g_2^{3/2,1}(\varrho,0)]^2+\frac{1}{2}[g_1^{1/2,2}(\varrho,0)]^2\right\}. \quad \text{(A25)}$$

The FWHM in the $z=0$ plane is then defined by $2\varrho_0$ with ϱ_0 such that

$$\frac{1}{2\pi}\int_0^{2\pi}|\mathbf{E}(\varrho_0,\varphi,0)|^2d\varphi=\frac{1}{2}|\mathbf{E}(\mathbf{0})|^2. \quad \text{(A26)}$$

The real part of the complex Poynting vector in cylindrical coordinates is

$$\mathrm{Re}\,S_\varrho(\mathbf{r})=\frac{1}{2}\mathrm{Re}[E_\varphi H_z^*-E_zH_\varphi^*]$$
$$=-\frac{\pi^2n^3f^2}{\lambda_0^2}\sqrt{\frac{\epsilon_0}{\mu_0}}\,\mathrm{Im}[(g_0^{1/2,1}+g_0^{3/2,1}-g_2^{1/2,1}+g_2^{3/2,1})(g_1^{1/2,2})^*], \quad \text{(A27)}$$

$$\mathrm{Re}\,S_\varphi(\mathbf{r})=\frac{1}{2}\mathrm{Re}[E_zH_\varrho^*-E_\varrho H_z^*]=0, \quad \text{(A28)}$$

$$\operatorname{Re} S_z(\mathbf{r}) = \frac{1}{2}\operatorname{Re}[E_\varrho H_\varphi^* - E_\varphi H_\varrho^*]$$
$$= \frac{\pi^2 n^3 f^2}{2\lambda_0^2}\sqrt{\frac{\epsilon_0}{\mu_0}}(|g_0^{1/2,1} + g_0^{3/2,1}|^2 - |g_2^{1/2,1} - g_2^{3/2,1}|^2). \tag{A29}$$

The total power flow P through a plane z=const is most easily calculated by substituting (A10) and (A11) into Eq. (29). One finds

$$P = \frac{\pi}{2} n f^2 \sqrt{\frac{\epsilon_0}{\mu_0}} \sin^2 \alpha_{\max}. \tag{A30}$$

We have along the z axis

$$g_1^{\nu,\mu}(0,z) = g_2^{\nu,\mu}(0,z) = 0,$$

for all ν and μ, and

$$g_0^{1/2,1}(0,z) = \int_0^{\alpha_{\max}} e^{ik_0 nz\cos\alpha}\cos^{1/2}\alpha\sin\alpha d\alpha$$
$$= \frac{e^{ik_0 nz}-1}{ik_0 nz} - \frac{e^{ik_0 nz\cos\alpha_{\max}}-1}{ik_0 nz}\cos^{1/2}\alpha_{\max}$$
$$- i\sqrt{\frac{\pi}{2}}\frac{\mathcal{C}[\sqrt{(2/\pi)k_0 nz\cos\alpha_{\max}}] - \sqrt{(2/\pi)k_0 nz\cos\alpha_{\max}} + i\mathcal{S}[\sqrt{(2/\pi)k_0 nz\cos\alpha_{\max}}]}{(k_0 nz)^{3/2}}$$
$$+ i\sqrt{\frac{\pi}{2}}\frac{\mathcal{C}[\sqrt{(2/\pi)k_0 nz}] - \sqrt{(2/\pi)k_0 nz} + i\mathcal{S}[\sqrt{(2/\pi)k_0 nz}]}{(k_0 nz)^{3/2}}, \tag{A31}$$

$$g_0^{1/2,1}(\varrho,-z) = g_0^{1/2,1}(\varrho,z)^*, \tag{A32}$$

where

$$\mathcal{C}(z) = \int_0^z \cos\left(\frac{\pi}{2}t^2\right)dt, \tag{A33}$$

$$\mathcal{S}(z) = \int_0^z \sin\left(\frac{\pi}{2}t^2\right)dt. \tag{A34}$$

Furthermore,

$$g_0^{3/2,1}(0,z) = \int_0^{\alpha_{\max}} e^{ik_0 nz\cos\alpha}\cos^{3/2}\alpha\sin\alpha d\alpha$$
$$= \frac{e^{ik_0 nz}-1}{ik_0 nz} - \frac{e^{ik_0 nz\cos\alpha_{\max}}-1}{ik_0 nz}\cos^{3/2}\alpha_{\max} + \frac{3}{2}\frac{e^{ik_0 nz}-1-ik_0 nz}{(k_0 nz)^2} - \frac{3}{2}\frac{e^{ik_0 nz\cos\alpha_{\max}}-1-ik_0 nz\cos\alpha_{\max}}{(k_0 nz)^2}\cos^{1/2}\alpha_{\max}$$
$$+ \frac{3}{2}\sqrt{\frac{\pi}{2}}\frac{\mathcal{C}(\sqrt{(2/\pi)k_0 nz\cos\alpha_{\max}}) - \sqrt{(2/\pi)k_0 nz\cos\alpha_{\max}}}{[(2/\pi)k_0 nz]^{5/2}}$$
$$+ i\frac{3}{2}\sqrt{\frac{\pi}{2}}\frac{\mathcal{S}[\sqrt{(2/\pi)k_0 nz\cos\alpha_{\max}}] - \frac{\pi}{6}[(2/\pi)k_0 nz\cos\alpha_{\max}]^{3/2}}{[(2/\pi)k_0 nz]^{5/2}}$$
$$- \frac{3}{2}\sqrt{\frac{\pi}{2}}\frac{\mathcal{C}[\sqrt{(2/\pi)k_0 nz}] - \sqrt{(2/\pi)k_0 nz} + i\left\{\mathcal{S}[\sqrt{(2/\pi)k_0 nz}] - \frac{\pi}{6}[(2/\pi)k_0 nz]^{3/2}\right\}}{[(2/\pi)k_0 nz]^{5/2}}, \tag{A35}$$

$$g_0^{3/2,1}(0,-z) = g_0^{3/2,1}(0,z)^*. \tag{A36}$$

In particular,

$$g_0^{1/2,1}(0,0) = \frac{2}{3}(1-\cos^{3/2}\alpha_{\max}), \tag{A37}$$

$$g_0^{3/2,1}(0,0) = \frac{2}{5}(1-\cos^{5/2}\alpha_{\max}). \tag{A38}$$

Hence, along the optical axis, the electric field is

$$\mathbf{E}(0,0,z) = \frac{i\pi nf}{\lambda_0}[g_0^{1/2,1}(0,z) + g_0^{3/2,1}(0,z)]\hat{\mathbf{x}}, \tag{A39}$$

and the electric energy density is

$$|\mathbf{E}(0,0,z)|^2 = |E_x(0,0,z)|^2 = \frac{\pi^2 n^2 f^2}{\lambda_0^2}|g_0^{1/2,1}(0,z) + g_0^{3/2,1}(0,z)|^2. \tag{A40}$$

In the focal point

$$|\mathbf{E}(0)|^2 = \frac{\pi^2 n^2 f^2}{\lambda_0^2}\left[\frac{16}{15} - \frac{2}{3}\cos^{3/2}\alpha_{\max} - \frac{2}{5}\cos^{5/2}\alpha_{\max}\right]^2. \tag{A41}$$

Now

$$\begin{aligned} g_0^{1/2,1}(0,z) + g_0^{3/2,1}(0,z) &= \int_0^{\alpha_{\max}} e^{ik_0 nz\cos\alpha}(\cos^{1/2}\alpha \\ &\quad + \cos^{3/2}\alpha)\sin\alpha d\alpha \\ &= 2\int_0^{\alpha_{\max}} e^{ik_0 nz\cos\alpha}\sin\alpha d\alpha + \mathcal{I}(z), \end{aligned} \tag{A42}$$

where

$$\mathcal{I}(z) = \int_0^{\alpha_{\max}} e^{ik_0 nz\cos\alpha}(\cos^{1/2}\alpha + \cos^{3/2}\alpha - 2)\sin\alpha d\alpha. \tag{A43}$$

For small numerical aperture

$$\begin{aligned} &\int_0^{\alpha_{\max}} e^{ik_0 nz\cos\alpha}\sin\alpha d\alpha \\ &= e^{i(k_0 nz/2)(1+\cos\alpha_{\max})}\frac{\sin\left[\frac{k_0 nz}{2}(1-\cos\alpha_{\max})\right]}{\frac{k_0 nz}{2}} \\ &= e^{i(k_0 nz/2)(1+\cos\alpha_{\max})}\frac{\sin\left(\frac{k_0 nz}{4}\alpha_{\max}^2\right)}{\frac{k_0 nz}{4}\alpha_{\max}^2}\frac{\alpha_{\max}^2}{2} + O(\alpha_{\max}^4), \end{aligned} \tag{A44}$$

where $O(\alpha_{\max}^4)$ denotes a term which modulus is smaller than $C\alpha_{\max}^4$, where C is a number that is independent of z. Furthermore, $\mathcal{I}(z)$ can be estimated as follows:

$$\begin{aligned} |\mathcal{I}(z)| &\leqslant \int_0^{\alpha_{\max}} (2-\cos^{1/2}\alpha - \cos^{3/2}\alpha)\sin\alpha d\alpha \\ &= 2(1-\cos\alpha_{\max}) - \frac{2}{3}(1-\cos^{3/2}\alpha_{\max}) \\ &\quad - \frac{2}{5}(1-\cos^{5/2}\alpha_{\max}) = O(\alpha_{\max}^4). \end{aligned} \tag{A45}$$

Hence,

$$\begin{aligned} |g_0^{1/2,1}(z,0) + g_0^{3/2,1}(z,0)|^2 &= \left[\frac{\sin\left(\frac{k_0 nz}{4}\alpha_{\max}^2\right)}{\frac{k_0 nz}{4}\alpha_{\max}^2}\right]^2 \alpha_{\max}^4 \\ &\quad + O(\alpha_{\max}^6). \end{aligned} \tag{A46}$$

The first term is identical to the intensity distribution along the optical axis in the scalar paraxial theory. This shows that when the numerical aperture is small, the focal depth of the intensity in the vectorial theory is the same as in the scalar paraxial theory.

[1] V. S. Ignatowsky, Trans. Opt. Inst. Petrograd **I**, paper IV (1919).
[2] V. S. Ignatowsky, Trans. Opt. Inst. Petrograd **I**, paper V (1919).
[3] E. Wolf, Proc. R. Soc. London, Ser. A **253**, 349 (1959).
[4] B. Richards and E. Wolf, Proc. R. Soc. London, Ser. A **253**, 358 (1959).
[5] X. S. Xie and R. C. Dunn, Science **265**, 361 (1994).
[6] L. Novotny, M. R. Beversluis, K. S. Youngworth, and T. G. Brown, Phys. Rev. Lett. **86**, 5251 (2001).
[7] Q. W. Zhan, Opt. Express **12**, 3377 (2004).
[8] L. E. Helseth, Opt. Commun. **212**, 343 (2002).
[9] M. Meier, V. Romano, and T. Feurer, Appl. Phys. A: Mater. Sci. Process. **86**, 329 (2007).
[10] N. Sanner, N. Huot, E. Audouard, C. Larat, J.-P. Huignard, and B. Loiseaux, Opt. Lett. **30**, 1479 (2005).
[11] B. M. I. van der Zande, J. Lub, H. J. Verhoef, W. P. M. Nijssen, and S. A. Lakehal, Liq. Cryst. **33**, 723 (2006).
[12] M. A. A. Neil, F. Massoumian, R. Juskaitis, and T. Wilson, Opt. Lett. **27**, 1929 (2002).
[13] M. Stalder and M. Schadt, Opt. Lett. **21**, 1948 (1996).
[14] I. Iglesias and B. Vohnsen, Opt. Commun. **271**, 40 (2007).
[15] H. P. Urbach and S. F. Pereira, Phys. Rev. Lett. **100**, 123904 (2008).
[16] R. Dorn, S. Quabis, and G. Leuchs, Phys. Rev. Lett. **91**, 233901 (2003).
[17] S. Quabis, R. Dorn, M. Eberler, O. Glöckl, and G. Leuchs, Opt. Commun. **179**, 1 (2000).

[18] S. Quabis, R. Dorn, M. Eberler, O. Glöckl, and G. Leuchs, Appl. Phys. B: Lasers Opt. **72**, 109 (2001).
[19] C. J. R. Sheppard and A. Choudhurry, Appl. Opt. **43**, 4322 (2004).
[20] C. Sanchez, University of Zaragoza, patent pending.
[21] I. Ekeland and R. Téman, *Convex Analysis and Variational Problems* (North-Holland, Amsterdam, 1976).
[22] D. G. Luenberger, *Optimization by Vector Space Methods* (Wiley, New York, 1969).
[23] A. P. Prudnikov, Yu. A. Brychkov, and O. I. Marichev, *Integrals and Series* (Gordon and Breach Science Publishers, New York, 1986), Vol. 1, p. 456.
[24] A. S. van de Nes, L. Billy, S. F. Pereira, and J. J. M. Braat, Opt. Express **12**, 1281 (2004).